






## Tissemouminites: A new group of primitive achondrites spanning the transition between acapulcoites and winonaites

A. STEPHANT <sup>1,2\*</sup>, C. CARLI <sup>1</sup>, M. ANAND<sup>2</sup>, A. NÉRI<sup>3</sup>, J. DAVIDSON <sup>4</sup>, G. PRATESI <sup>1,5</sup>,  
T. CUPPONE<sup>5</sup>, R. C. GREENWOOD<sup>2</sup>, and I. A. FRANCHI <sup>2</sup>

<sup>1</sup>Istituto di Astrofisica e Planetologia Spaziali – INAF, Rome 00133, Italy

<sup>2</sup>School of Physical Sciences, The Open University, Milton Keynes MK7 6AA, UK

<sup>3</sup>Bayerisches Geoinstitut, University of Bayreuth, Bayreuth 95447, Germany

<sup>4</sup>Buseck Center for Meteorite Studies, School of Earth and Space Exploration, Arizona State University, Tempe, Arizona 85287, USA

<sup>5</sup>Dipartimento di Scienze della Terra, Università degli Studi di Firenze, Firenze 50121, Italy

\*Corresponding author. E-mail: alice.stephant@inaf.it

(Received 03 August 2022; revision accepted 28 November 2022)

**Abstract**—The Northwest Africa (NWA) 090 meteorite, initially classified as an acapulcoite, presents petrological, chemical, and isotopic characteristics comparable to a group of seven primitive winonaites: Dhofar 1222, NWA 725, NWA 1052, NWA 1054, NWA 1058, NWA 1463, and NWA 8614. Five of these samples were previously classified as acapulcoites or ungrouped achondrites before being reclassified as winonaites based on their oxygen isotopic compositions. These misclassifications are indicative of the particular compositional nature of these primitive achondrites. All contain relict chondrules and a lower closure temperature of metamorphism of  $820 \pm 20$  °C compared to other typical winonaites, as well as mineral elemental compositions similar to those of acapulcoites. The oxygen isotopic signature of these samples,  $\delta^{17}\text{O}$  of  $1.18 \pm 0.17\%$ ,  $\delta^{18}\text{O}$  of  $3.18 \pm 0.30\%$ , and  $\Delta^{17}\text{O}$  of  $-0.47 \pm 0.02$ , is in fact resolvable from both acapulcoites and winonaites. We investigate the relationship between these eight primitive achondrites, typical winonaites, and acapulcoites, to redefine petrological, mineralogical, and geochemical criteria of primitive achondrite classification. Distinguishing between winonaites, acapulcoites, and this group of eight primitive achondrites can be unambiguously done using a combination of several mineralogical and chemical criteria. A combination of olivine fayalite content and FeO/MnO ratio, as well as plagioclase potassium content allow us to separate these three groups without the absolute necessity of oxygen isotope analyses. NWA 090 as well as the other seven primitive achondrites, although related to winonaites, are most likely derived from a parent body distinct from winonaites and acapulcoites–lodranites, and define a new group of primitive achondrites that can be referred to as tissemouminites.

### INTRODUCTION

Acapulcoites–lodranites and winonaites are primitive achondrites (Prinz et al., 1983), meaning they have crystalline igneous, hence achondritic, textures, but with near-chondritic bulk compositions (Krot et al., 2014; Weisberg et al., 2006). These meteorites have sampled partially melted chondritic parent bodies, formed only a few Ma after the formation of calcium–aluminum inclusions (CAIs; Schulz et al., 2010). As such, they provide a window into the early stages of protoplanetary

differentiation. Acapulcoites and lodranites most likely originated from a single chondritic parent body, close in composition to H ordinary chondrites (McCoy, Keil, Clayton, et al., 1997; Mittlefehldt, 2014; Palme et al., 1981). These primitive achondrites represent residues of different degrees of partial melting of their chondritic precursor that occurred in a moderately reducing environment (Keil & McCoy, 2018). Lodranites were heated to higher temperatures (1100–1250 °C), resulting in a coarse-grained texture (540–700  $\mu\text{m}$ ) and in 5%–10% of Fe,Ni–FeS cotectic and basaltic partial melting. Migration of these

melts has been observed through the depletion of troilite and plagioclase in some lodranites relative to acapulcoites. Acapulcoites are finer grained achondrites (150–230  $\mu\text{m}$ ), as they were heated to lower temperatures (950–1050  $^{\circ}\text{C}$ ), producing lower degrees of Fe,Ni–FeS cotectic partial melting (1%–4%) without any melt migration. Hence, these meteorites kept a chondritic mineralogy and bulk composition (Floss, 2000; McCoy et al., 1996; McCoy, Keil, Clayton, et al., 1997; McCoy, Keil, Muenow, et al., 1997; Mittlefehldt et al., 1996; Palme et al., 1981; Patzer et al., 2004). Winonaites are generally more fine-grained than acapulcoites (90–250  $\mu\text{m}$ ; Zeng et al., 2019); experienced limited Fe,Ni–FeS partial melting, if any (900–1200  $^{\circ}\text{C}$ ); and show evidence for brecciation and high metamorphism (similar to type 6 chondrites) on the chondritic precursor body (Benedix et al., 1998, 2005). While the chondritic mineralogy is similar between winonaites and acapulcoites, the winonaite precursor would have formed in a more reduced environment than the acapulcoite–lodranite parent body, with the major element composition lying between enstatite chondrites and H ordinary chondrites (Benedix et al., 1998; Kimura et al., 1992) and similarities in trace element abundances to CM carbonaceous chondrites (Hunt et al., 2017). However, chondritic precursors of both winonaites and acapulcoites–lodranites are unlike any known chondritic groups and our best witnesses for primitive achondrite parent bodies are relict chondrule-bearing samples (Rubin, 2007; Schrader et al., 2017; Zeng et al., 2019). These relict chondrule-bearing samples have been suggested to be called “chondritic acapulcoites” (Neumann et al., 2018). As such this nomenclature, as well as the term “chondritic winonaites,” will be used in the text for simplicity.

To date, 9 of 69 classified winonaites (as of May 2022) contain relict chondrules: Dhofar 1222; Pontlyfni; Mont Morris (Wisconsin); Northwest Africa (NWA) 725, NWA 1463; NWA 1052 and its pairs NWA 1054; and NWA 8614 (Benedix et al., 1998, 2003; Cecchi & Caporali, 2015; Farley et al., 2015; Néri, 2019; Rubin, 2007; Zeng et al., 2019). One should note that Mount Morris is an ambiguous member of this subgroup; while this meteorite is often cited as containing relict chondrules in the literature (Benedix et al., 1998; Greenwood et al., 2012; Schrader et al., 2017), Benedix et al. (1998) actually identified only one suspected chondrule, while Davis et al. (1977), Graham et al. (1977), and Bevan and Grady (1988) did not report any. Moreover, Bevan and Grady (1988) concluded that Mount Morris (Wisconsin) is a detached silicate inclusion from the IAB iron Pine River. Therefore, Mount Morris will not be considered further in this article. Interestingly, from the eight chondritic winonaites, only Pontlyfni, NWA 1463, and NWA 8614 were originally classified in the *Meteoritical Bulletin* as winonaites. Dhofar 1222, NWA 1052, and NWA 1054

were initially classified as acapulcoites as their mineralogy and chemistry seemed consistent with these primitive achondrites, while NWA 1058 and NWA 725 were classified as ungrouped achondrites. Recently, these samples have been reclassified as winonaites based on their oxygen isotope compositions (Greenwood et al., 2012; Zeng et al., 2019) or cosmic ray exposure (CRE) ages that do not match with the restricted 4–7 Ma CRE age of the acapulcoite–lodranite clan (Eugster & Lorenzetti, 2005). These somehow regular misclassifications highlight two important points: (i) the need to revise the mineralogical and geochemical distinguishing criteria between winonaite and acapulcoite primitive achondrites, some of which are obviously outdated, and (ii) the peculiar nature of this group of chondritic winonaites.

Modal abundance, mineralogy, and chemistry are typically used to distinguish acapulcoites from winonaites (Benedix et al., 1998; Kimura et al., 1992; Yugami et al., 1998); lodranites, being coarser grained, are readily identified from the two previously mentioned groups. Compositions of mafic minerals are generally used to classify primitive achondrites into either the acapulcoite or winonaite groups. A correlated variation plot between ferrosilite (Fs) content of low-Ca pyroxene and fayalite (Fa) content of olivine in primitive achondrites is often used for this purpose. Criteria to distinguish winonaites from acapulcoites include: (i) highly reduced assemblage, among which typically Mg-rich olivine and Mg-rich pyroxene, as well as the presence of highly reduced accessory minerals such as alabandite, daubr elite, and schreibersite; (ii) modal abundance of metal, troilite, and olivine; (iii) major element composition of pyroxene and chromite; (iv) bulk composition (Floss, 2000); and (v) oxygen isotopes (Clayton & Mayeda, 1996; Greenwood et al., 2012, 2017). Because the latter is not always measured to classify a meteorite (e.g., Keil & McCoy [2018] report that more than 50% of classified acapulcoites are lacking oxygen isotopic data), meteoriticists rely mostly on these mineralogy and chemistry criteria. However, acapulcoites and winonaites share many common characteristics making their distinction rather delicate, and the rise of primitive achondrite discoveries over the last 20 years has exposed the limit of mineralogical and geochemical distinguishing criteria. This is the case of some acapulcoites that are highly reduced ( $\text{Fa} < 7$  mole%) such as Allan Hills (ALH/ALHA) 81187 and ALH 84190, which is suspected to be its pair, as well as Superior Valley (SuV) 014, NWA 13041, NWA 13839, NWA 4816, and NWA 090. While ALHA 81187 and ALH 84190 have acapulcoite oxygen isotope signatures, the other five samples lack this information. Hence, a reclassification might be required.

Most chondritic winonaites exhibit an abnormal oxidized state compared to typical winonaites

(Fa > 5.2 mole% and/or Fs > 7.1 mole%): Dhofar 1222, NWA 725, NWA 1052 and its pairs NWA 1054, NWA 1058, NWA 1463, and NWA 8614. Several studies have already noted the primitive nature of these chondritic winonaites (Benedix et al., 2003; Farley et al., 2015; Floss et al., 2008; Irving & Rumble, 2006; Néri, 2019; Zeng et al., 2019). In fact, they are all characterized by a protogranular very fine-grained texture, the presence of relatively abundant relict chondrules, higher oxidation state compared to typical winonaites, and a low temperature of metamorphism. In fact, these criteria are indicative of a lack of igneous fractionation processes, otherwise observed in other typical winonaites. Most likely, they sampled the regolith of the winonaite parent body (Floss et al., 2008; Zeng et al., 2019), direct proxy of the chondritic precursor, being the least heated zone of parental bodies. Interestingly, these samples have been suggested likely to be paired and to be named W chondrites (Irving & Rumble, 2006). In fact, it has been recently highlighted that distinction between highly metamorphosed chondrites and primitive achondrites is vague (Tomkins et al., 2020) and chondritic achondrites are transitional between strongly metamorphosed chondrites and primitive achondrites (Greenwood et al., 2012).

Here, we investigate the petrography, mineralogy, chemistry, and isotopic compositions of NWA 090, classified as an acapulcoite (Bouvier et al., 2017), as well as a group of seven primitive winonaites, namely Dhofar 1222, NWA 725, NWA 1052, NWA 1054, NWA 1058, NWA 1463, and NWA 8614 (five of them previously classified as acapulcoites or ungrouped achondrites). These meteorites lie between acapulcoites and winonaites, highlighting the need to revisit the classification criteria of primitive achondrites. Our data indicate a new group of primitive achondrites, likely derived from a parent body different to those of acapulcoite–lodranite and winonaite, despite sharing similar oxygen isotope characteristics as that of winonaites. We suggest naming this new group tisseumouninites after the location where the type specimen NWA 725 was found.

## SAMPLE AND ANALYTICAL TECHNIQUES

### Samples

Northwest Africa 090 was purchased in Erfoud, Morocco in 2000 (Bouvier et al., 2017). NWA 090 shows medium weathering and low shock and a well-developed fusion crust. Several rounded mineral aggregates were identified as well as a radial pyroxene aggregate. NWA 090 was then classified as an acapulcoite based on its mineral major element composition. We study here the same polished thin section of NWA 090 used for the first

classification, prepared at Buseck Center for Meteorite Studies, Arizona State University. Northwest Africa 1052 and its pair NWA 1054 section from the Department of Earth Sciences, Firenze, were also analyzed as some mineral chemical composition about these samples were lacking.

### Secondary Electron Microscope and Electron Probe Microanalyses

Polished thin section of NWA 090 was studied using optical and scanning electron microscopy (SEM) methods. Microscopic observations under transmitted and reflected light performed at IAPS sample preparation facility were used to determine the main mineral phases and study the presence of relict chondrules. Backscattered electron (BSE) images of minerals and relict chondrules were obtained with the ZEISS EVO MA15 SEM (MEMA Center, University of Firenze). Elemental X-ray maps of Al, Ca, Cr, Cu, Fe, K, Mg, Mn, Na, Ni, P, S, Si, and Ti were collected to identify pyroxene, olivine, feldspar, phosphate, troilite, chromite, taenite, kamacite, and accessory minerals in NWA 090. Chemical characterization of olivine and pyroxene in NWA 090 was obtained using the Cameca SX-100 electron microprobe at the University of Arizona. Chemical characterization of all silicate minerals (olivine, pyroxene, feldspar) and opaques (troilite, chromite, taenite, and kamacite) was carried out with the JEOL JXA 8230 (Department of Earth Sciences, University of Firenze). Using the Cameca SX-100 electron microprobe at the University of Arizona, quantitative olivine analyses were performed in wavelength-dispersive mode, with an accelerating potential of 15 kV. A focused beam of 20 nA was used to analyze pyroxenes. Quantitative mineral analyses done with the JEOL JXA 8230 were performed in wavelength-dispersive mode, with an accelerating potential of 15 kV. ZAF correction was applied to all measurements. Typical detection limits were 0.02%–0.05% for major element oxide abundances. Mineral modal abundances were calculated using XMapTools (Lanari et al., 2014).

### Thermodynamic Modeling

Closure temperatures were determined using geothermometers based on two different mineral pairs. We used both chromite–olivine and two-pyroxene systems to determine temperatures, using the MELTS calculator (Sack & Ghiorso, 1991). Oxygen fugacity was calculated from both these closure temperatures using quartz–iron–fayalite (QIFa) and quartz–iron–ferrosilite (QIFs) equilibria, as in Gardner-Vandy et al. (2012).

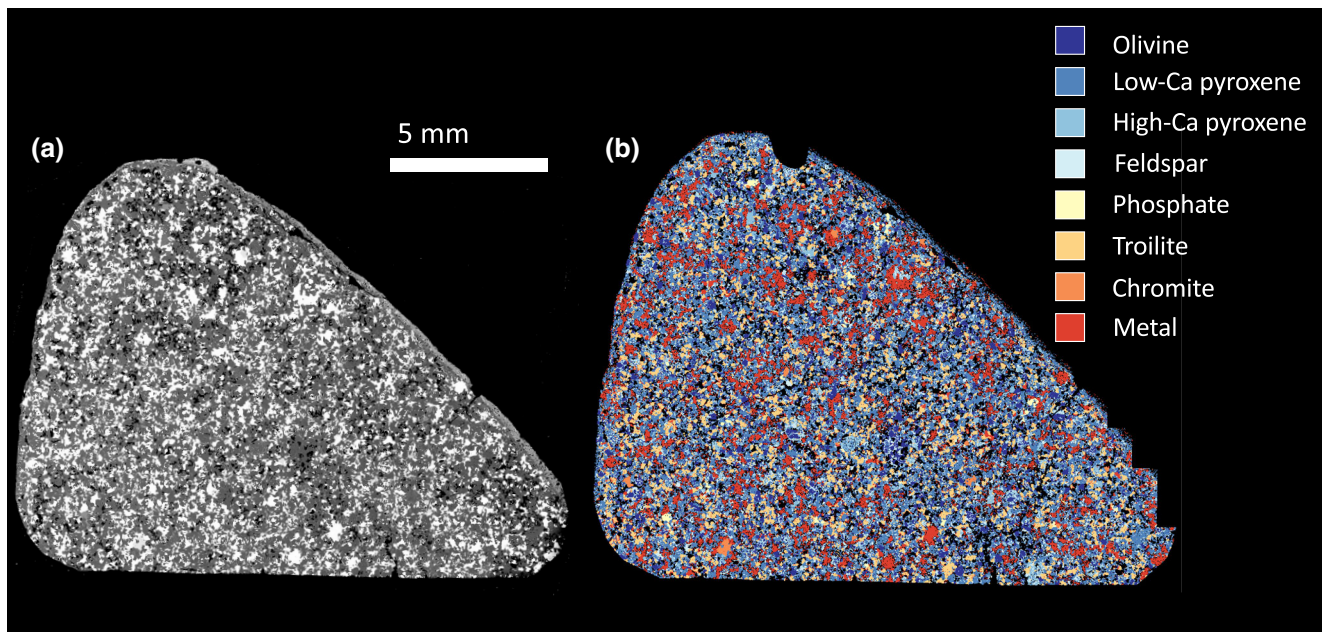


Fig. 1. a) Backscattered electron (BSE) maps of NWA 090 thin section. b) X-ray map generated with XMapTools software of NWA 090. Phases are identified in X-ray map with the color assigned in the legend. Metal consists of FeNi metal phases and terrestrial oxidation products. This map was used to determine the modal abundances of mineral phases for NWA 090.

### Laser Fluorination—Oxygen Isotope Analyses

Oxygen isotope analysis was performed at the Open University (OU), using an infrared laser-assisted fluorination system (Greenwood et al., 2017) on NWA 090. Oxygen was released from the sample (approximate weight of 2 mg) by heating in the presence of BrF<sub>5</sub>. The released oxygen gas was purified by passing it through two cryogenic nitrogen traps and over a bed of heated KBr. Oxygen gas was analyzed using a MAT 253 dual inlet mass spectrometer. Recent levels of precision obtained on the OU system, as demonstrated by 38 analyses of an in-house obsidian standard, were as follows: 0.053‰ for δ<sup>17</sup>O; 0.095‰ for δ<sup>18</sup>O; 0.018‰ for Δ<sup>17</sup>O (2 SD) (Starkey et al., 2016). Oxygen isotope analyses are reported in standard delta notation. The δ<sup>18</sup>O value is calculated as  $\delta^{18}\text{O} = \left( \frac{[^{18}\text{O}/^{16}\text{O}]_{\text{sample}}}{[^{18}\text{O}/^{16}\text{O}]_{\text{ref}}} - 1 \right) \times 1000$  (‰). The δ<sup>17</sup>O value is calculated as  $\delta^{17}\text{O} = \left( \frac{[^{17}\text{O}/^{16}\text{O}]_{\text{sample}}}{[^{17}\text{O}/^{16}\text{O}]_{\text{ref}}} - 1 \right) \times 1000$  (‰). The reference for both is Vienna Standard Mean Ocean Water VSMOW. The deviation from the terrestrial fractionation line has been calculated using the linearized format of Miller et al. (2002):  $\Delta^{17}\text{O} = 1000 \times \ln(1 + \delta^{17}\text{O}/1000) - k1000 \ln(1 + \delta^{18}\text{O}/1000)$  where  $k$  is 0.5247. The sample was pretreated with ethanolamine thioglycolate (EATG) solution to remove terrestrial weathering products.

### RESULTS

#### Petrography

NWA 090, which retains a well-developed fusion crust (Figs. 1 and 2a), displays a protogranular texture, with typical curvilinear grain boundaries between olivine and other silicates (Mercier & Nicolas, 1975) and a lack of 120° triple junctions. The sample is dominated by olivine, low-Ca pyroxene, FeNi metal, and troilite. The granoblastic texture as well as the high amount of opaque phases in NWA 090 (consisting of metal, troilite, chromite, and oxidation products) is clearly noticeable from the BSE map of the thin section (Fig. 1). Terrestrial weathering products are present, resulting in oxidation of FeNi metallic phases, mostly around grains surrounded by porosity or through small cracks (few micrometers; e.g., Fig. 2c). We estimated the amount of terrestrial weathering products at 8.9 wt%. Hence, a W2 weathering grade, indicating a moderate oxidation of metal, is justified (Bouvier et al., 2017; Wlotzka, 1993). The average silicate grain size was uniformly ~80 μm, smaller than the 200 μm initially reported in the *Meteoritical Bulletin* (Bouvier et al., 2017). Holly-leaf-shaped Fe-Ni metal grains and troilite (dominantly occurring as single crystal) are largely present in the section, as well as few well-crystallized chromite grains

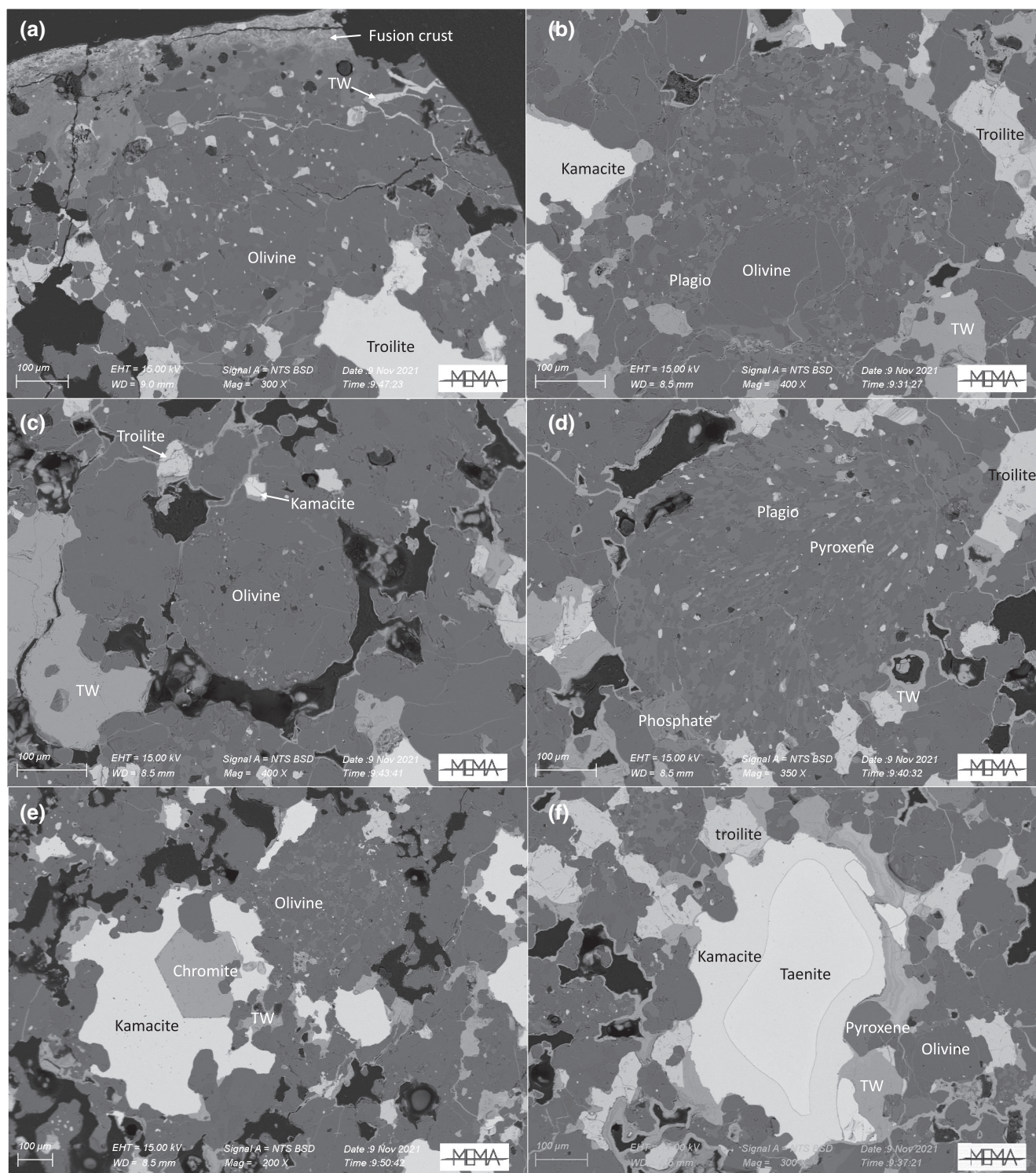


Fig. 2. BSE images of NWA 090 highlighting various features: a) relict porphyritic olivine chondrule near the fusion crust of NWA 090, (b) large relict porphyritic olivine chondrule, (c) rounded relict porphyritic olivine chondrule. Identification of relict chondrules was aided by the presence of voids around almost all relict chondrules. Notice also patches and veins of terrestrial alteration products, oxidized metallic phases (TW). d) Large relict radial pyroxene chondrule. Most chondrules also contain small blebs of opaque phases. e) Chromite grain in contact with kamacite and a relict chondrule. f) Kamacite overgrowth on a taenite grain. The taenite–kamacite interface is marked by a large Ni spike (cf. Fig. 8).

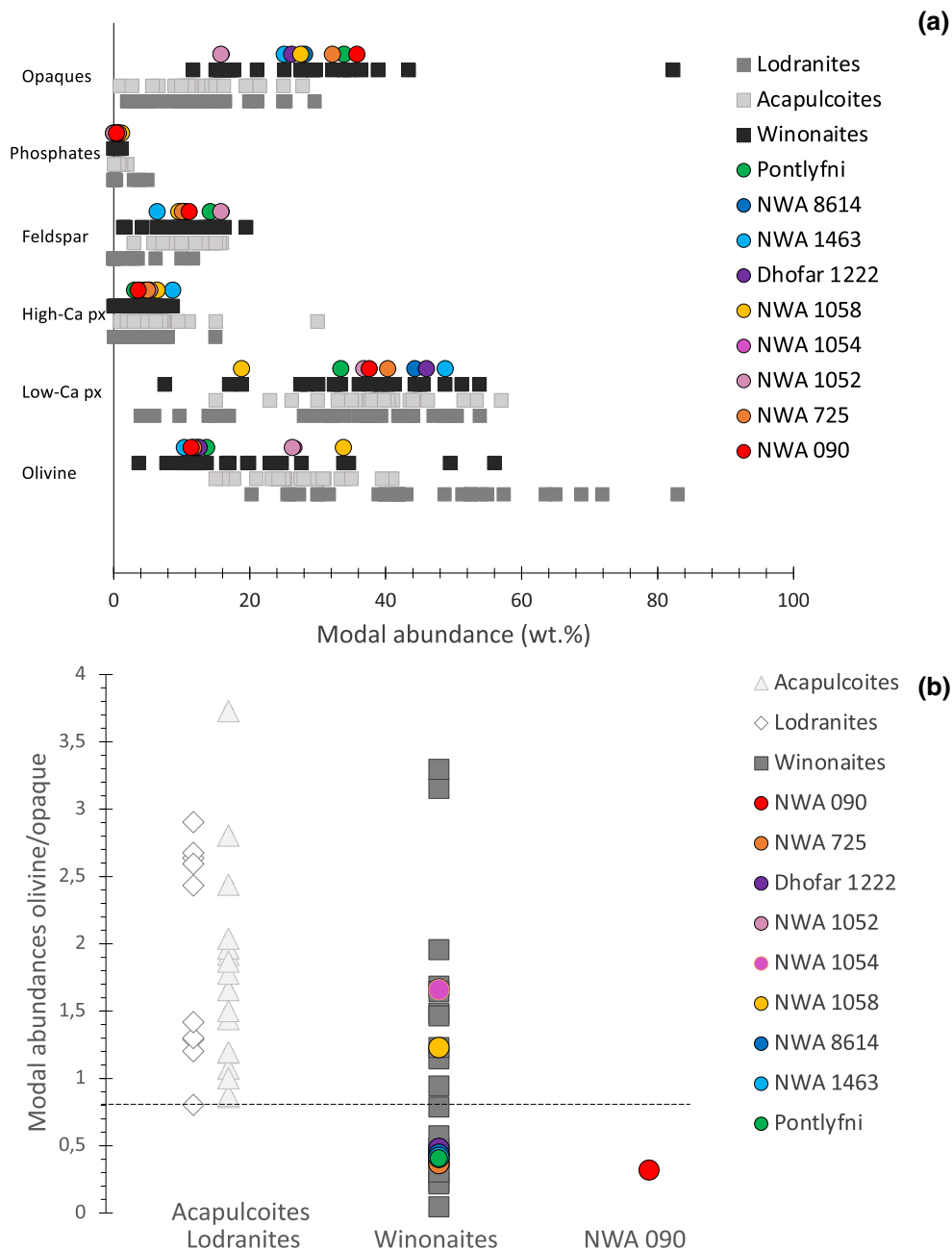


Fig. 3. a) Modal abundances of acapulcoites, lodranites, winonaites, chondritic winonaites, and NWA 090. Modal abundances of chondritic winonaites are expressed in Table 2. b) Olivine/opaque modal abundances ratio for acapulcoites, winonaites, chondritic winonaites, and NWA 090. The Y-axis ends at 4 for clarity, but some acapulcoites show higher olivine/opaque modal abundance ratio up to 37. No acapulcoites show a ratio lower than 0.8 (dashed line). Data on acapulcoites are from Keil and McCoy (2018) and references therein. Data on winonaites are from Zeng et al. (2019) and references therein. References for the chondritic winonaites are listed in Table 1.

(Fig. 2e). However, typical Fe,Ni-FeS veins are absent from the section. Porosity in NWA 090 is estimated to be 8% (using ImageJ program), mostly surrounding relict chondrules and grain boundaries (e.g., Fig. 2e).

Modal abundances of NWA 090 have been calculated with XMapTools software (Lanari et al., 2014)

based on X-ray maps (Fig. 3; Table 1) (wt%): 11.4 olivine, 37.6 low-Ca pyroxene, 3.6 high-Ca pyroxene, 11.1 feldspar, 0.4 phosphates, 12.9 troilite, 0.5 chromite, 22.4 FeNi metallic phases. Some accessory mineral phases indicative of highly reducing conditions, such as daubreelite ( $\text{FeCr}_2\text{S}_4$ ), alabandite ( $\text{MnS}$ ), and

Table 1. Modal abundances of winonaites containing relict chondrules.

Samples	Opx	Ol	Pl	Cpx	Php	Tro	Chr	Metal	Acc.	Silicate	Opaque	References
NWA 725	40.3	11.8	10.1	5	0.7	10.3	0.9	21	—	67.9	32.2	Zeng et al. (2019)
NWA 1058	18.8	33.8	9.6	6.4	1.2	7	0.4	20.1	—	68.6	27.5	Cecchi and Caporali (2015)
NWA 1052	36.8	26.3	15.8	5.3	—	6.2	0.1	9.5	—	84.2	15.8	Cecchi and Caporali (2015)
NWA 1054	37.4	26.7	16	5.3	0.4	7.5	0.5	8.5	—	85.2	16.1	Cecchi and Caporali (2015)
Dhofar 1222	46	12.6	10.5	3.8	0.8	10.7	0.7	14.8	—	73.7	26.2	Néri (2019)
NWA 090	37.6	11.4	11.1	3.6	0.4	12.9	0.5	22.4	tr.	64.1	35.8	This study
NWA 8614	44.3	12.3	10.1	4.6	0.7	6.9	0.4	20.4	0.38	72.0	28.1	Farley et al. (2015)
Pontlyfni	33.4	13.7	14.2	3.1	—	21	—	12.9	2.1	64.4	33.9	Hunt et al. (2017)
NWA 1463	48.8	10.4	6.4	8.7	0.4	8.8	0.3	16	0.1	74.3	25.1	Hunt et al. (2017)
Range of winonaites												
Min	7.5	3.7	1.4	0	0	1.8	0	2.3	0	16.7	11.7	Zeng et al. (2019) and references therein
Max	53.8	56	15.5	8.7	1.2	21	1	80.5	2.1	88.3	82.3	

Range of modal abundances for typical winonaite is given for comparison. Tr. for trace as few grains of schreibersite have been identified in NWA 090 section. One should note that modal abundance estimations were done with diverse methods.

Table 2. Summary of silicate chemical compositions of winonaites with relict chondrules.

Samples	Ol Fa	Ol FeO/ MnO		Opx Fs	Opx Wo	Cpx Fs	Cpx Wo	An	Ab	Or	References
NWA 725	6.6	13.4	7.9	1.5	3.1	46.5	12.4	82.5	5.1	Zeng et al. (2019)	
NWA 1058	6.1	11.7	7.7	1.3	3.3	46.1	13.4	81.2	5.4	Patzer et al. (2004)	
NWA 1052	6.0	—	7.6	1.4	3.6	45.3	13.7	79.9	6.4	Metbull	
NWA 1054	6.4	—	7.8	1.3	3.3	45.4	14.3	79.5	6.3	Metbull	
Dhofar 1222	6.6	13.2	7.7	1.3	3.9	45.6	13.3	80.7	6.0	Néri (2019)	
NWA 090	6.1	12.9	7.4	1.3	3.2	45.4	12.2	82.2	5.3	This study	
ISD	0.2	0.8	0.3	0.4	0.2	0.6	0	0.1	0.1	This study	
NWA 8614	6.5	13	7.8	1.4	3.5	45.5	13.6	79.9	6.4	Farley et al. (2015)	
Pontlyfni	1.1	4.8	1.2	1.6	1.1	46.1	—	—	—	Benedix et al. (1998)	
NWA 1463	3.2	—	7.4	1.2	—	—	12.6	82.8	4.6	MetBull	

schreibersite ( $[\text{Fe,Ni}]_3\text{P}$ ), were not found. These are typically found in winonaites and enstatite chondrites, while rarely in acapulcoites (Benedix et al., 1998). Only a few schreibersite grains were found in NWA 090.

Finally, 12 relict chondrules were also identified in the section (Fig. 2a–e), with an average diameter of  $\sim 400 \mu\text{m}$  (from 150 to 700  $\mu\text{m}$ ). Most of them are easily identifiable as they have retained their primary textures. We estimate that 83% of relict chondrules are porphyritic, mainly olivine-rich, porphyritic olivine (PO) chondrules (Fig. 2a–c and 2e). One large radial pyroxene chondrule has been identified (Fig. 2d) as well as a probable granular olivine chondrule. Relict chondrules represent about 1.5 vol% of the thin section studied here.

## Mineral Major Elemental Compositions

### Silicates

Composition summary and detailed electron microprobe analysis data for silicate phases in NWA 090 and other chondritic winonaites are reported in Tables 2 and 3, respectively, and presented in Figs. 4–6. Olivine

fayalite (Fa) content is  $6.1 \pm 0.2$  and FeO/MnO  $12.9 \pm 0.8$  ( $n = 11$ ) (Figs. 4 and 5). The composition of low-Ca pyroxene is homogeneous, with ferrosilite (Fs) content of  $7.4 \pm 0.3$ , wollastonite (Wo) content of  $1.3 \pm 0.4$ , and FeO/MnO of  $9.8 \pm 1.3$  ( $n = 18$ ) (Figs. 4 and 6). The Fs and Fa compositions of NWA 090 lie toward the higher range for winonaites and place NWA 090 in the overlapping zone with acapulcoites values (Fig. 4), leading to some confusion in classifying this meteorite. High-Ca pyroxene composition is Fs  $3.2 \pm 0.2$  and Wo  $45.4 \pm 0.6$ , with a  $\text{Cr}_2\text{O}_3$  content of  $1.18 \pm 0.04 \text{ wt}\%$  and an  $\text{Na}_2\text{O}$  content of  $0.70 \pm 0.02 \text{ wt}\%$  ( $n = 11$ ) (Fig. 6). Interestingly, relict chondrules are often enriched in high-Ca pyroxenes compared with the matrix. Plagioclase in NWA 090 is enriched in the orthoclase component compared to typical winonaites, with an average composition of  $\text{An}_{12.2}\text{Ab}_{82.2 \pm 0.1}\text{Or}_{5.3 \pm 0.1}$  (Fig. 6).

### Opaques

Detailed electron microprobe analysis data for opaque phases in NWA 090 and other chondritic winonaites are

Table 3. Average olivine, low-Ca pyroxene, high-Ca pyroxene, and plagioclase chemical compositions of winonaites with relict chondrules.

Samples	SiO <sub>2</sub>	TiO <sub>2</sub>	Al <sub>2</sub> O <sub>3</sub>	Cr <sub>2</sub> O <sub>3</sub>	FeO	MnO	MgO	CaO	Na <sub>2</sub> O	K <sub>2</sub> O	Total	References
<b>Olivine</b>												
NWA 725	41.6	bdl	bdl	bdl	6.44	0.48	51.2	0.03	bdl	bdl	99.85	Zeng et al. (2019)
NWA 1058	40.65	bdl	bdl	bdl	6.07	0.52	52.07	bdl	bdl	bdl	99.31	Patzer et al. (2004)
NWA 1052	41.7	0.03	bdl	0.26	5.27	0.49	54.38	0.01	bdl	bdl	102.17	This study
NWA 1054	40.57	0.04	0.01	0.18	5.58	0.51	54.72	0.04	bdl	bdl	101.55	This study
Dhofar 1222	41.72	bdl	bdl	bdl	6.48	0.49	51.58	bdl	bdl	bdl	100.28	Néri (2019)
NWA 090	40.79	bdl	bdl	0.09	6.09	0.47	52.30	bdl	bdl	bdl	99.73	This study
1SD	0.32			0.14	0.21	0.03	0.25				0.28	
NWA 8614	—	—	—	—	—	—	—	—	—	—	—	—
Pontlyfni	42.7	bdl	bdl	bdl	0.77	0.16	56.9	bdl	bdl	bdl	100.53	Benedix et al. (1998)
NWA 1463	—	—	—	—	—	—	—	—	—	—	—	—
<b>Low-Ca pyroxene</b>												
NWA 725	58.6	0.16	0.21	0.2	5.35	0.58	34.4	0.78	0.02	bdl	100.3	Zeng et al. (2019)
NWA 1058	56.91	0.15	0.23	0.23	5.30	0.59	35.32	0.71	0.03	0.00	99.47	Patzer et al. (2004)
NWA 1052	57.98	0.18	0.26	0.26	5.03	0.56	36.39	0.77	0.03	0.01	100.37	This study
NWA 1054	57.78	0.17	0.51	0.23	4.93	0.56	35.67	0.74	0.12	0.02	100.73	This study
Dhofar 1222	58.28	0.13	0.24	0.24	5.29	0.57	35.08	0.71	bdl	bdl	100.56	Néri (2019)
NWA 090	56.46	0.15	0.23	0.23	5.28	0.54	36.43	0.70	0.01	bdl	100.04	This study
1SD	3.84	0.04	0.06	0.06	0.43	0.03	3.85	0.20	0.01	bdl		
NWA 8614	—	—	—	—	—	—	—	—	—	—	—	—
Pontlyfni	59.2	bdl	0.34	bdl	0.33	bdl	39.4	0.76	bdl	bdl	100.03	Benedix et al. (1998)
NWA 1463	—	—	—	—	—	—	—	—	—	—	—	—
<b>High-Ca pyroxene</b>												
NWA 725	55.5	0.58	0.69	1.02	2.11	bdl	17.4	22.4	0.71	bdl	100.4	Zeng et al. (2019)
NWA 1058	53.48	0.52	0.68	1.18	2.07	0.30	17.74	22.5	0.71	bdl	99.22	Patzer et al. (2004)
NWA 1052	54.24	0.56	0.68	1.22	2.11	0.29	18.49	22.15	0.75	0.01	100.48	This study
NWA 1054	54.24	0.55	0.67	1.19	2.21	0.29	18.24	22.03	0.71	0.01	100.13	This study
Dhofar 1222	54.31	0.5	0.66	1.18	2.43	0.26	17.59	22.07	0.70	bdl	99.7	Néri (2019)
NWA 090	53.85	0.56	0.68	1.18	2.00	0.25	17.93	22.04	0.70	bdl	99.19	This study
1SD	0.74	0.04	0.01	0.04	0.14	0.03	0.13	0.33	0.02	bdl		
NWA 8614	—	—	—	—	—	—	—	—	—	—	—	—
Pontlyfni	55	0.4	0.58	bdl	0.36	bdl	19.5	23.4	0.35	bdl	99.55	Benedix et al. (1998)
NWA 1463	—	—	—	—	—	—	—	—	—	—	—	—
<b>Plagioclase</b>												
NWA 725	64.6	0.06	22.1	0.1	0.49	bdl	0.03	2.51	9.23	0.87	99.99	Zeng et al. (2019)
NWA 1058	65.68	0.05	23.43	bdl	0.42	bdl	0.55	2.73	9.15	0.93	102.94	Patzer et al. (2004)
NWA 1052	—	—	—	—	—	—	—	—	—	—	—	—
NWA 1054	—	—	—	—	—	—	—	—	—	—	—	—
Dhofar 1222	64.97	bdl	21.06	bdl	0.67	bdl	bdl	2.8	9.44	1.06	100	Néri (2019)
NWA 090	64.97	0.07	21.99	bdl	0.27	bdl	0.01	2.63	9.84	0.95	100.73	This study
1SD												
NWA 8614	—	—	—	—	—	—	—	—	—	—	—	—
Pontlyfni	—	—	—	—	—	—	—	—	—	—	—	—
NWA 1463	—	—	—	—	—	—	—	—	—	—	—	—

bdl = below detection limit.

reported in Table 4. FeNi metal is mainly represented by kamacite. Taenite is also present and a crystal of taenite with an overgrowth of kamacite was found in the section (Fig. 2f). Ni profiles across the taenite–kamacite show an Ni spike of about 5 wt% in the taenite that occurs at the flat taenite/kamacite interface (Fig. 7). Kamacite nucleation and growth around a taenite matrix occurred upon cooling (Wood, 1967) and can be used as

metallographic cooling rate of the sample. The NWA 090 cooling rate was determined using the taenite central Ni content method (also known as the Wood method). We used the cooling rate curves calculated in ordinary chondrites by Willis and Goldstein (1981) and extrapolated by Taylor et al. (1987), in a similar manner as done by Scott et al. (2014b). Considering a taenite half-width of ~80 µm with a central Ni concentration of 17.5 wt%, we



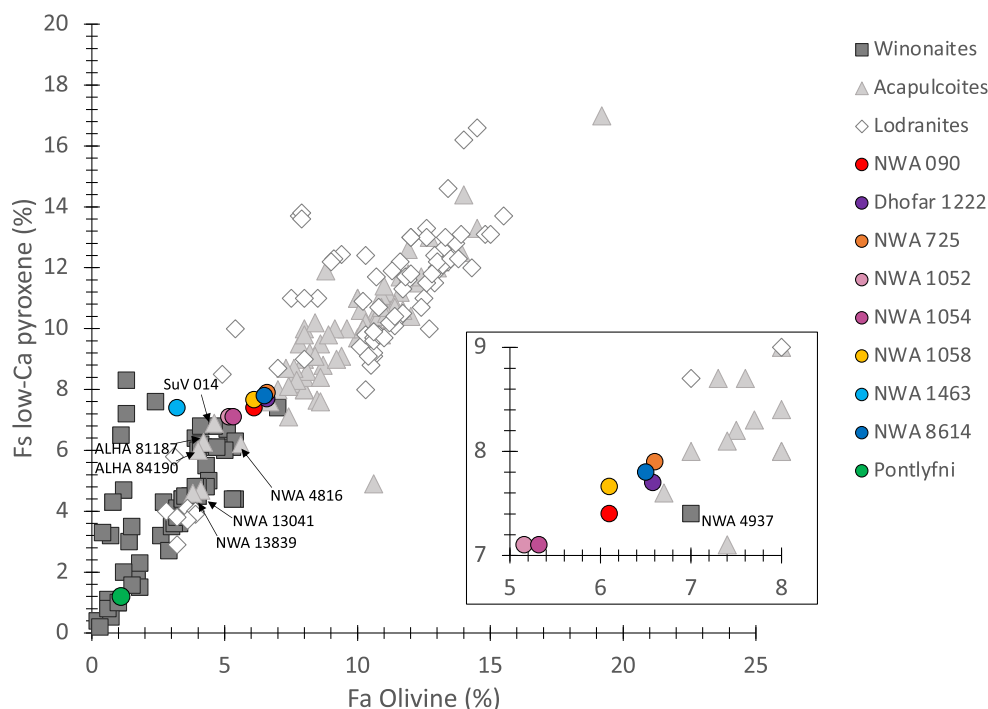


Fig. 4. Fa in olivine versus Fs in low-Ca pyroxene. Winonaites, acapulcoites, and lodranites form a trend. Chondritic winonaites are represented by filled circles. The winonaites as well as acapulcoites–lodranites generally have lower Fa in olivine than Fs in low-Ca pyroxene. This is indicative of solid-state reduction during cooling and consistent with the lower diffusion rates in low-Ca pyroxene relative to olivine (Huebner & Nord, 1981). Based on oxygen isotopes, NWA 4937 is indeed a winonaite while ALHA 81187 and ALH 84190 are acapulcoites, despite their contradictory Fa versus Fs (see text for details). Note that Pontlyfni, while having relict chondrules, does not match the composition of the other chondritic winonaites. Data on acapulcoites are from Keil and McCoy (2018) and references therein and the *Meteoritical Bulletin*; data on winonaites are from the *Meteoritical Bulletin*. Data on chondritic winonaites and references are listed in Table 2.

estimated a cooling rate for NWA 090 of about  $100 \text{ }^\circ\text{C Myr}^{-1}$ . The only sulfides in NWA 090 are troilite. Cr and Ni were below the detection limit. Well-crystallized chromite is also present (Fig. 2e) and shows an enrichment in  $\text{V}_2\text{O}_3$  compared to typical winonaites, with an average of  $0.52 \pm 0.07 \text{ wt}\%$ , as well as an enrichment in iron compared to winonaites, with FeO content of  $16.92 \pm 0.50 \text{ wt}\%$  (Fig. 8). The presence of taenite (Fig. 2f) as well as well-crystallized oxidized mineral like chromite, and no trace of typical highly reduced accessory minerals like daubr elite and alabandite are indicative of NWA 090 being FeO-rich compared to winonaites (Benedix et al., 1998; Li et al., 2011; McCoy et al., 1996; Patzer et al., 2004; Yugami et al., 1998).

### Thermodynamic Modeling

The closure temperatures and corresponding oxygen fugacities for both olivine–chromite and two-pyroxene systems are presented in Table 5 and Fig. 9. Two-pyroxene thermometry for NWA 090 yields a closure temperature of  $827 \text{ }^\circ\text{C}$ . For comparison, we also recalculated the temperature of Dhofar 1222, NWA 1058, and NWA 725,

which yield similar temperatures of  $818 \text{ }^\circ\text{C}$ ,  $805 \text{ }^\circ\text{C}$ , and  $831 \text{ }^\circ\text{C}$ , respectively. The olivine–chromite thermometry of NWA 090 gives a temperature of  $657 \text{ }^\circ\text{C}$ . Similarly, Dhofar 1222, NWA 1058, and NWA 725 temperatures were estimated at  $657 \text{ }^\circ\text{C}$ ,  $640 \text{ }^\circ\text{C}$ , and  $649 \text{ }^\circ\text{C}$ , respectively. The lower temperature recorded by the olivine–chromite system is consistent with Fe–Mg exchange between these minerals closing at lower temperature than Ca-transfer between pyroxenes. The olivine–chromite oxygen fugacity recorded by the four sections ranges from 2.56 to 2.49 log units below the iron–wustite (IW) oxygen buffer, with an average  $-2.53 \pm 0.05$  log units. The pyroxene oxygen fugacity ranges from 2.17 to 2.14 log below the IW buffer, with an average  $-2.16 \pm 0.03$  log units. Olivine–chromite and two-pyroxene thermometers exhibit a strong correlation among the four samples.

### Oxygen Isotopic Composition

The oxygen isotopic composition of NWA 090 and other samples is presented in Fig. 10 and in Table 6, along with other primitive achondrites with relict chondrules. Analysis of NWA 090 by laser fluorination

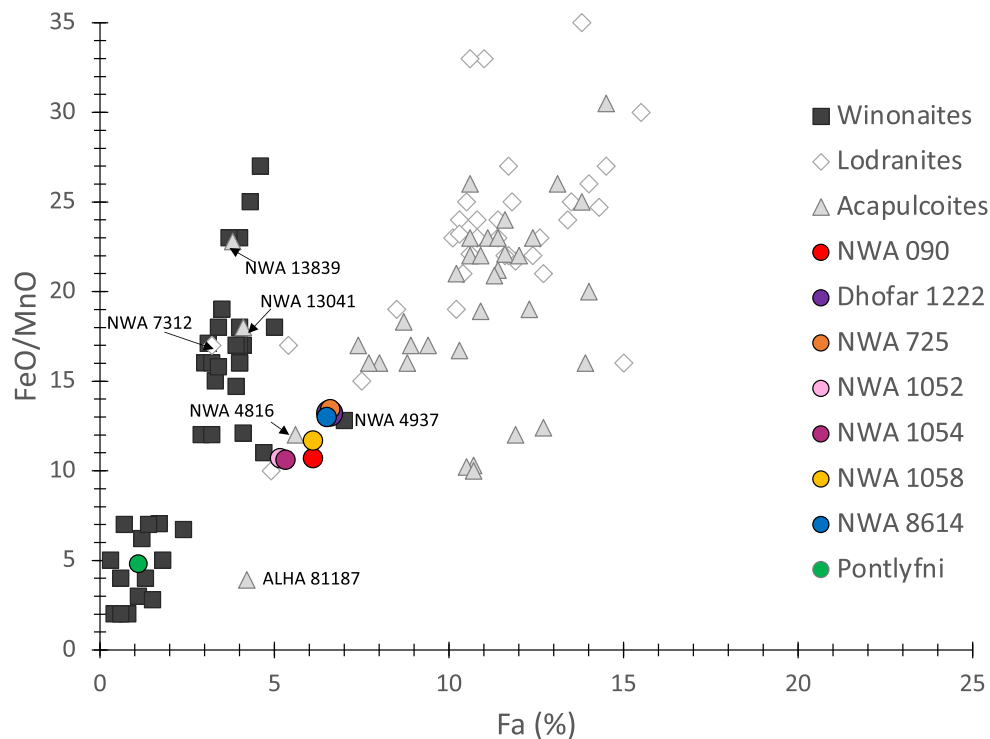


Fig. 5. Fayalite content versus FeO/MnO in olivine of acapulcoites, lodranites, and winonaites. Acapulcoites–lodranites and winonaites define two distinct trends. The chondritic winonaites fit on the acapulcoites–lodranites trend (see text for details). Data on acapulcoites are from Keil and McCoy (2018) and references therein and the *Meteoritical Bulletin*; data on winonaites are from the *Meteoritical Bulletin*. Data on chondritic winonaites and references are listed in Table 2. Note here that NWA 13839 and NWA 13041, classified as acapulcoites, fit on the winonaite trend, as well as lodranite NWA 7312. Similarly, winonaite NWA 4937 fits on the acapulcoite–lodranite trend. These samples might need reclassification (see text for details).

gave  $\delta^{17}\text{O} = +1.12$ ,  $\delta^{18}\text{O} = +3.32$ , and  $\Delta^{17}\text{O} = -0.46$ .  $\delta^{18}\text{O}$  and  $\delta^{17}\text{O}$  lie on the fractionation line of winonaites, although values are lower. Oxygen isotopic composition of NWA 090 is similar to those of Dhofar 1222, NWA 725, NWA 1052, NWA 1054, NWA 1058, NWA 1463, and NWA 8614.

## DISCUSSION

### Northwest Africa 090 and Other Chondritic Winonaites in the Winonaite–Acapulcoite Dichotomy: A New Group of Primitive Achondrites

The petrographic, chemical, and isotopic characteristics of NWA 090 conflict with the traditional dichotomy between acapulcoites and winonaites. In fact,

most of NWA 090's characteristics are ambiguous. Petrographically, NWA 090 displays typical curvilinear grain boundaries between olivine and other silicates and a lack of  $120^\circ$  junctions. These two features suggest less extensive solid-state recrystallization in NWA 090 than typical winonaites, which usually exhibit equigranular textures and abundant triple junctions (Benedix et al., 1998). The average  $80\ \mu\text{m}$  silicate grain size measured in NWA 090 is also typically lower than in winonaites (Zeng et al., 2019), and within the range of other chondritic winonaites, that is, Dhofar 1222 and NWA 725 ( $\sim 45$  to  $55\ \mu\text{m}$ ; Néri, 2019). The characteristics of easily identified relict chondrules are similar to those in H chondrites and chondritic acapulcoites (Friedrich et al., 2015; Gooding & Keil, 1981; Scott & Krot, 2014), with a diameter range of  $400\ \mu\text{m}$  (OCs:  $450\ \mu\text{m}$ ;

Fig. 6. Composition of low-Ca pyroxene (a), high-Ca pyroxene (b–d), and plagioclase (e) in NWA 090 compared to winonaites, acapulcoites, and other chondritic winonaites. a) FeO versus MnO content of low-Ca pyroxene. b)  $\text{Cr}_2\text{O}_3$  versus  $\text{Na}_2\text{O}$  contents (wt%) of high-Ca pyroxenes. c) Mg# versus  $\text{Al}_2\text{O}_3$  contents (wt%) of high-Ca pyroxenes. d) Mg# versus  $\text{Cr}_2\text{O}_3$  contents (wt%) of high-Ca pyroxenes. e) Plagioclase AnAbOr composition. Acapulcoite data are from Keil and McCoy (2018) and references therein. Winonaite data are from Zeng et al. (2019), Kimura et al. (1992), Benedix et al. (1998), Yugami et al. (1998), and Li et al. (2011). References and composition of silicate minerals of the chondritic winonaites are listed in Table 3.

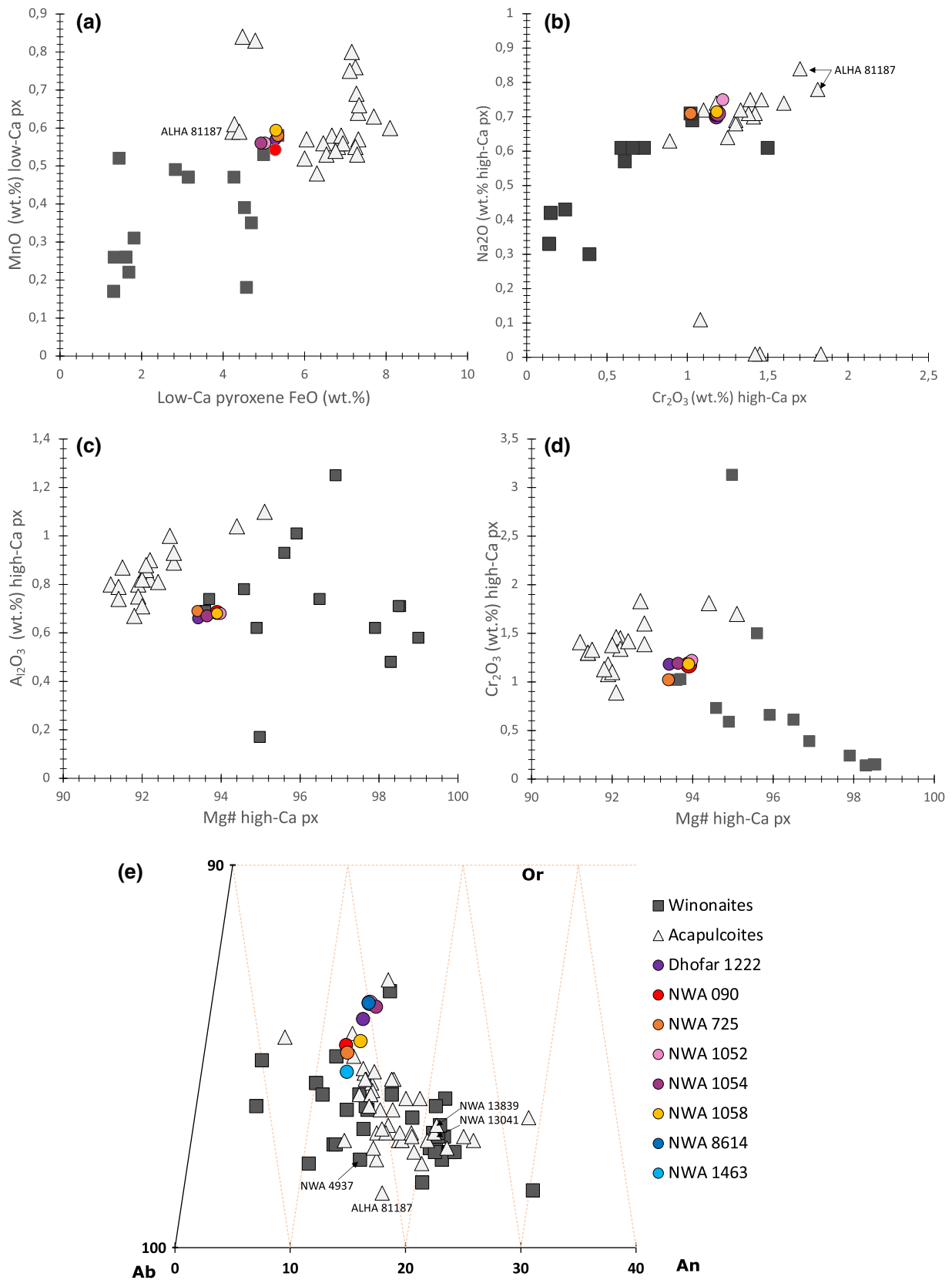


Table 4. Average kamacite, taenite, troilite, and chromite chemical composition of NWA 090 and some winonaite with relic chondrules.

	Kamacite NWA 090	Taenite NWA 090	Troilite NWA 090
Fe	92.07 ± 0.60	75.62 ± 9.25	63.15 ± 0.06
Ni	6.93 ± 0.10	23.39 ± 8.39	0.01 ± 0.02
Mn	—	—	0.01 ± 0.01
S	—	—	37.36 ± 0.07
Cu	—	—	0.03 ± 0.03
Total	99.00 ± 0.60	99.01 ± 0.86	100.56 ± 0.07

Chromite	NWA 090	NWA 725	Dhofar 1222	NWA 1058
TiO <sub>2</sub>	0.87 ± 0.12	0.86	0.89	0.93
Al <sub>2</sub> O <sub>3</sub>	3.10 ± 1.40	5.2	5.39	5.29
V <sub>2</sub> O <sub>3</sub>	0.52 ± 0.07	0.53	0.52	—
Cr <sub>2</sub> O <sub>3</sub>	65.71 ± 1.71	64.56	63.7	64.89
FeO	16.92 ± 0.50	16.31	16.24	16.34
MnO	2.49 ± 0.41	2.47	2.26	2.56
MgO	8.56 ± 0.68	9.12	9.36	9.34
Total	98.17 ± 0.58	99.07	98.4	99.35

Data on NWA 725 and Dhofar 1222 are from Néri (2019); data on NWA 1058 are from Patzer et al. (2004).

acapulcoites: 400–700 μm; Friedrich et al., 2015) and a greater abundance of porphyritic relict chondrules.

As for most of the winonaite, low-Ca pyroxene is the most abundant mafic silicate, consistent with the reduced nature of winonaite compared to ordinary chondrites (Benedix et al., 1998). The modal abundances of NWA 090 and its olivine/opaque ratio (Fig. 3) are evocative of winonaite (Cecchi & Caporali, 2015; Hunt et al., 2017; Zeng et al., 2019). The overlapping of Fs and Fa signatures between NWA 090 and acapulcoites (Fig. 4) and the presence of taenite and the absence of other highly reduced accessory minerals attest to NWA 090 being less reduced and more FeO-rich than typical winonaite. Interestingly, chemical elemental compositions of low-Ca and high-Ca pyroxenes set NWA 090 in the overlapping zone between winonaite and acapulcoite (Fig. 6). Low-Ca pyroxene in NWA 090 has an MnO content of 0.54 wt%, closer to the acapulcoite range (0.48–0.84 wt%) than to the winonaite range (0.17–0.53 wt%) (cf. Fig. 6a) (Benedix et al., 1998; Keil & McCoy, 2018; Kimura et al., 1992; Li et al., 2011; Yugami et al., 1998; Zeng et al., 2019). Similarly, high-Ca pyroxene in NWA 090 has an Na<sub>2</sub>O content of 0.70 wt%, also within the acapulcoite range (0.63–0.84 wt%) rather than the winonaite range (0.30–0.69 wt%), apart from Tierra Blanca at 1.51 wt% (cf. Fig. 6b and references therein). However, when plotting Al<sub>2</sub>O<sub>3</sub> or Cr<sub>2</sub>O<sub>3</sub> of high-Ca pyroxene versus its Mg# (Mg/

[Mg + Fe]), NWA 090 seems to fit better in the winonaite compositional field (Fig. 6c and 6d). The compositions of both olivine and chromite set NWA 090 clearly in the acapulcoite compositional field. Plotting the fayalite content versus its FeO/MnO ratio, two trending lines define remarkably the winonaite clan and the acapulcoite–lodranite clan (Fig. 5). NWA 090 sits on the acapulcoite trend rather than on the winonaite trend, consistent with its initial classification as acapulcoite (Bouvier et al., 2017). Vanadium content of chromite delimits acapulcoite and winonaite clans, with a limit value of 0.4 wt% (Fig. 8). Indeed, acapulcoites range from 0.44 to 1.03 wt% V<sub>2</sub>O<sub>3</sub> (Keil & McCoy, 2018), while winonaite range from 0.03 to 0.38 wt% V<sub>2</sub>O<sub>3</sub> (Benedix et al., 2005; Kimura et al., 1992). With a V<sub>2</sub>O<sub>3</sub> content of 0.52 ± 0.07, NWA 090 is clearly within the acapulcoite field (Fig. 8). Finally, plagioclase compositions in NWA 090 seem to differ from both acapulcoites and winonaite, with a higher average Or content of 5.3 ± 0.1 compared to 3.6 ± 1.0 and 3.2 ± 1.2, for acapulcoites and winonaite, respectively (Fig. 6e and references therein).

Interestingly, most of NWA 090's features match those of other classified chondritic winonaite, that is Dhofar 1222, NWA 725, NWA 1052, NWA 1054, NWA 1058, NWA 1463, NWA 8614 (Figs. 3–6, 8). It is critical to note the special case of Pontlyfni regarding the other classified winonaite with relict chondrules. Pontlyfni does not fit with the other eight samples for any criteria (e.g., petrography, mineralogy, chemistry, or isotopy). In fact, the relict chondrules in Pontlyfni are not straightforward to identify (Benedix et al., 1998) and were not even identified by Graham et al. (1977), while relict chondrules in the other samples are numerous (1.5–5 vol%) and barely altered (Cecchi & Caporali, 2015; Farley et al., 2015; Rubin, 2007; Zeng et al., 2019). As such, it seems that Pontlyfni does not belong to this particular “chondritic achondrite” group and might be the only real winonaite-bearing relict chondrule. In terms of modal abundances, Dhofar 1222, NWA 1052, NWA 8614, NWA 1463, and NWA 725 have an olivine/opaque ratio below 0.8 (Fig. 3), concordant with NWA 090 and a winonaite affiliation. NWA 1058, NWA 1052, and its pair NWA 1054 do not concur with the other chondritic winonaite. However, the large range of modal abundances among the typical winonaite indicate that the parent body of winonaite must have been heterogeneous (Floss et al., 2008; Hunt et al., 2017). As such, this criterion cannot be used to exclude samples from a primitive achondrite group. Interestingly, NWA 1058 has been suggested to be paired with NWA 725, NWA 1052, NWA 1054, and NWA 1463 (Irving & Rumble, 2006). However, regarding the variations in modal abundances among these samples (Table 1), we

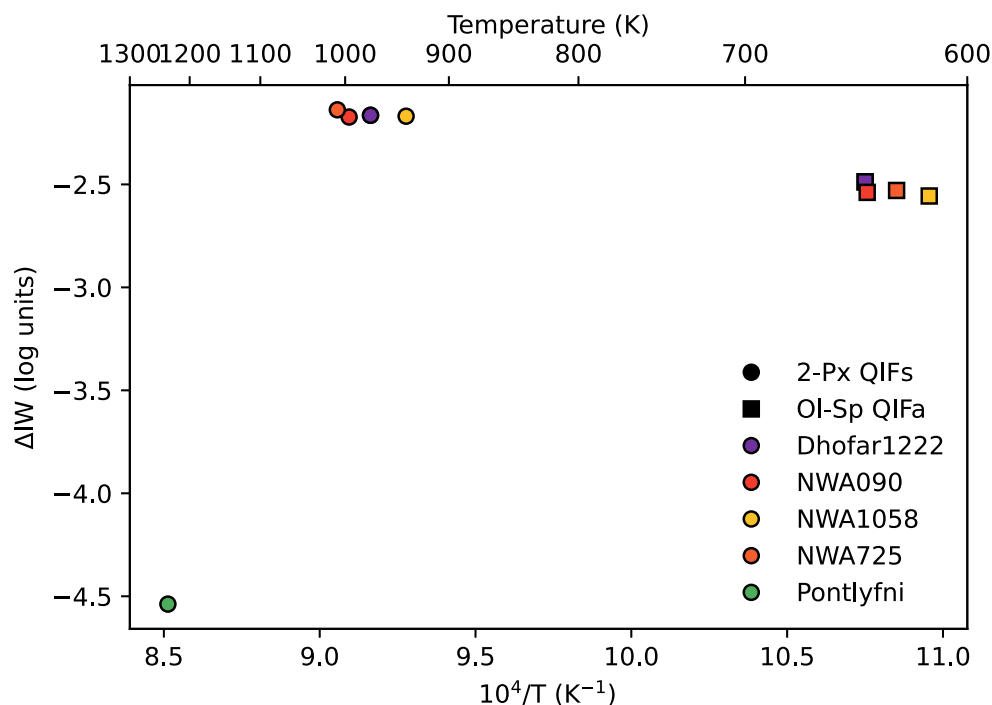


Fig. 7. Closure temperature of NWA 090, Dhofar 1222, NWA 725, NWA 1058, and Pontlyfni calculated based on low-Ca and high-Ca pyroxene thermometry and olivine–chromite thermometry.

argue against such a pairing, favoring a common parent body origin. Nonetheless, these eight samples match extremely well for all the other criteria of composition (Figs. 3–6 and 8; Tables 2 and 3).

The estimated closure temperature of 830 °C for NWA 090 (Fig. 9) as well as the absence of sulfide veins indicate that this primitive achondrite is one of the least thermally metamorphosed samples from primitive achondrites, since most winonaites and acapulcoites record metamorphic temperatures higher than 950 °C (Benedix et al., 1998; Hunt et al., 2017), between the Fe, Ni–FeS cotectic temperature (Kullerud, 1963) and the basaltic partial melting temperature (Morse, 1980). As such, NWA 090 did not experience any silicate partial melting. Dhofar 1222, NWA 725, and NWA 1058 recorded similar closure temperatures (Fig. 9), between 805 and 830 °C, while Farley et al. (2015) estimated a closure temperature at ~820 to 860 °C for NWA 8614. The lack of Fe veins, Ni-metal, and troilite indicates that NWA 1463 did not reach the Fe,Ni–FeS cotectic (Hunt et al., 2017). While two-pyroxene thermometry likely gives a closure temperature lower than the actual peak temperature of metamorphism (Benedix et al., 1998), it seems that none of the chondritic winonaites experienced any partial melting. Given these recorded temperatures, the oxygen fugacity for the grouplet of chondritic winonaites is estimated from two-pyroxene thermometry at  $2.16 \pm 0.03$  log units below the IW oxygen buffer and

between winonaites and acapulcoites (Wadhwa, 2008). Indeed, winonaites and silicate inclusions in IAB irons range from 2.3 to 3.2 log units below the Fe–FeO buffer (Benedix et al., 2005) while acapulcoites range from –1.85 to –3.09 log units (Benedix & Lauretta, 2006; Righter et al., 2016). The closure temperatures recorded by these samples are rather similar to the H5/H6 ordinary chondrite range of peak temperatures (Huss et al., 2006; McSween et al., 2002). Criteria of Van Schmus and Wood (1967) to determine the petrologic type of chondrite involve, among others, heterogeneity of silicate minerals based on the PMD (percent mean deviation) of FeO content, the presence of well-crystallized feldspar (Kovach & Jones, 2010), and the presence of taenite and texture of chondrules (Huss et al., 2006). The presence of chondrules that are readily delineated, a homogenous olivine composition (PMD = 2.5) and slightly heterogenous pyroxene composition (PMD = 5.1) argue for a type 5 for NWA 090, similar to that inferred for NWA 1463 (Floss et al., 2008; Hunt et al., 2017), while the presence of taenite and abundant plagioclase >50  $\mu\text{m}$  (modal abundance 11.1%) is indicative of a highly metamorphosed chondrite closer to a type 6, similar to that inferred for NWA 8614 (Farley et al., 2015). As a matter of fact, Irving and Rumble (2006) inferred that NWA 1054 was a chondrite type 5/6 related to the winonaites and suggested to call these samples W chondrites. In their metamorphic facies series for

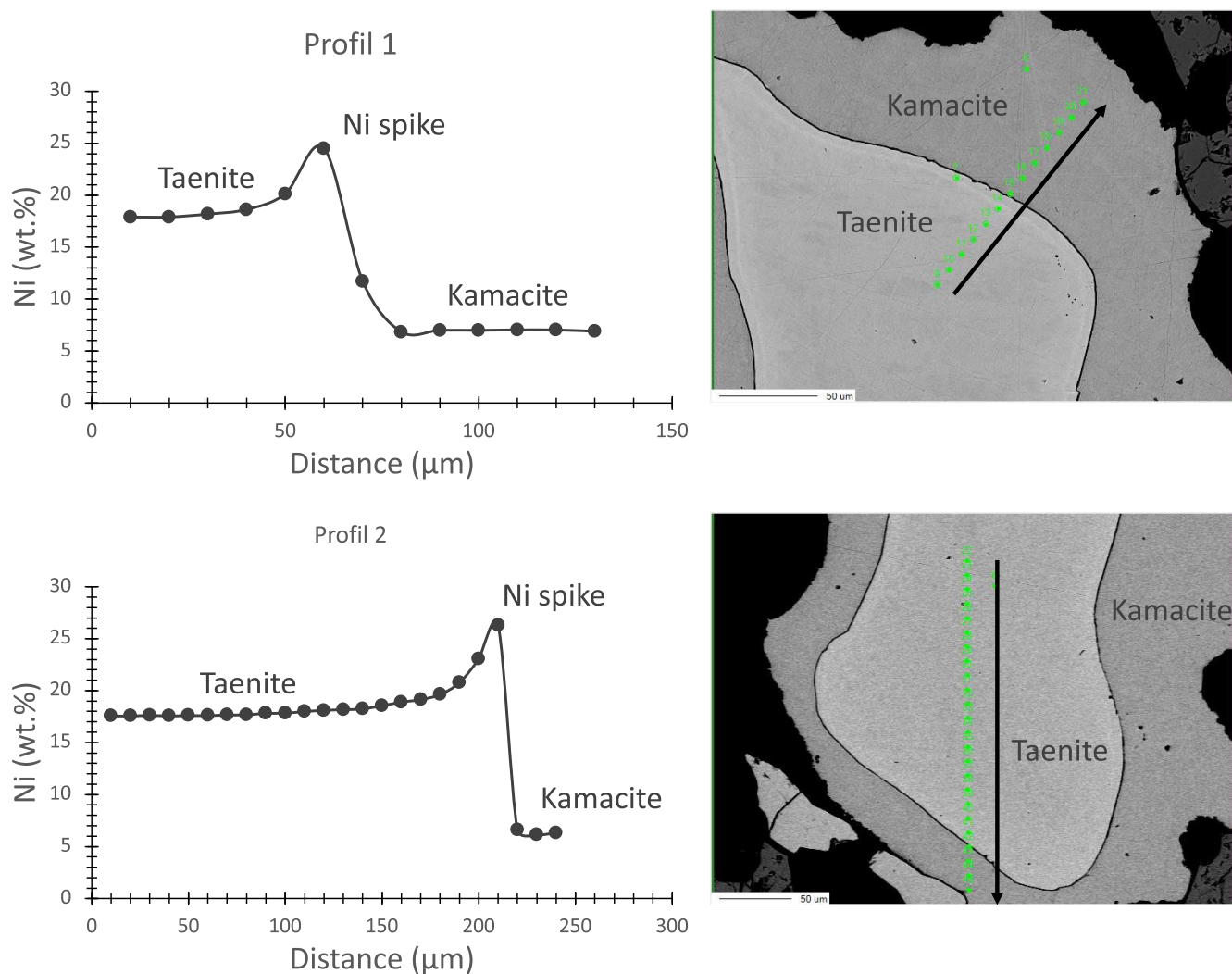


Fig. 8. Two different microprobe Ni traverses across the taenite–kamacite intergrowth. An Ni spike occurs at the flat taenite/kamacite interface.

Table 5. Thermodynamic properties determined for this study using data from Tables 3 and 4 for Dhofar 1222, NWA 090, NWA 1058, NWA 725.

Meteorite	Olivine–chromite Temperature (°C)	QIFa log( $f_{O_2}$ )	$\Delta$ IW	Two-pyroxene Temperature (°C)	QIFs log( $f_{O_2}$ )	$\Delta$ IW	$\Delta T$
Dhofar 1222	657	−25.4	−2.49	818	−20.7	−2.16	161
NWA 090	657	−25.5	−2.54	827	−20.5	−2.17	170
NWA 1058	640	−26.1	−2.56	805	−21.0	−2.17	165
NWA 725	649	−25.7	−2.53	831	−20.3	−2.14	182
Average	651	−25.7	−2.53	820	−20.6	−2.16	170
2SD	14	0.5	0.05	20	0.5	0.03	18

equilibrated stony meteorites, Tomkins et al. (2020) showed that NWA 725 falls within the plagioclase facies, meaning that it has equilibrated sufficiently to grow plagioclase over 10 µm in size, but has not yet undergone silicate partial melting. They also estimated this facies to be equivalent to petrologic types 5 and 6. The pristine

characteristic of these samples has already been suggested: Benedix et al. (2003) and Floss et al. (2008) highlighted the unique features of NWA 1463 compared to common winonaite, in particular bulk and trace element abundances, and inferred that it sampled the winonaite chondritic precursor. Equally, Zeng

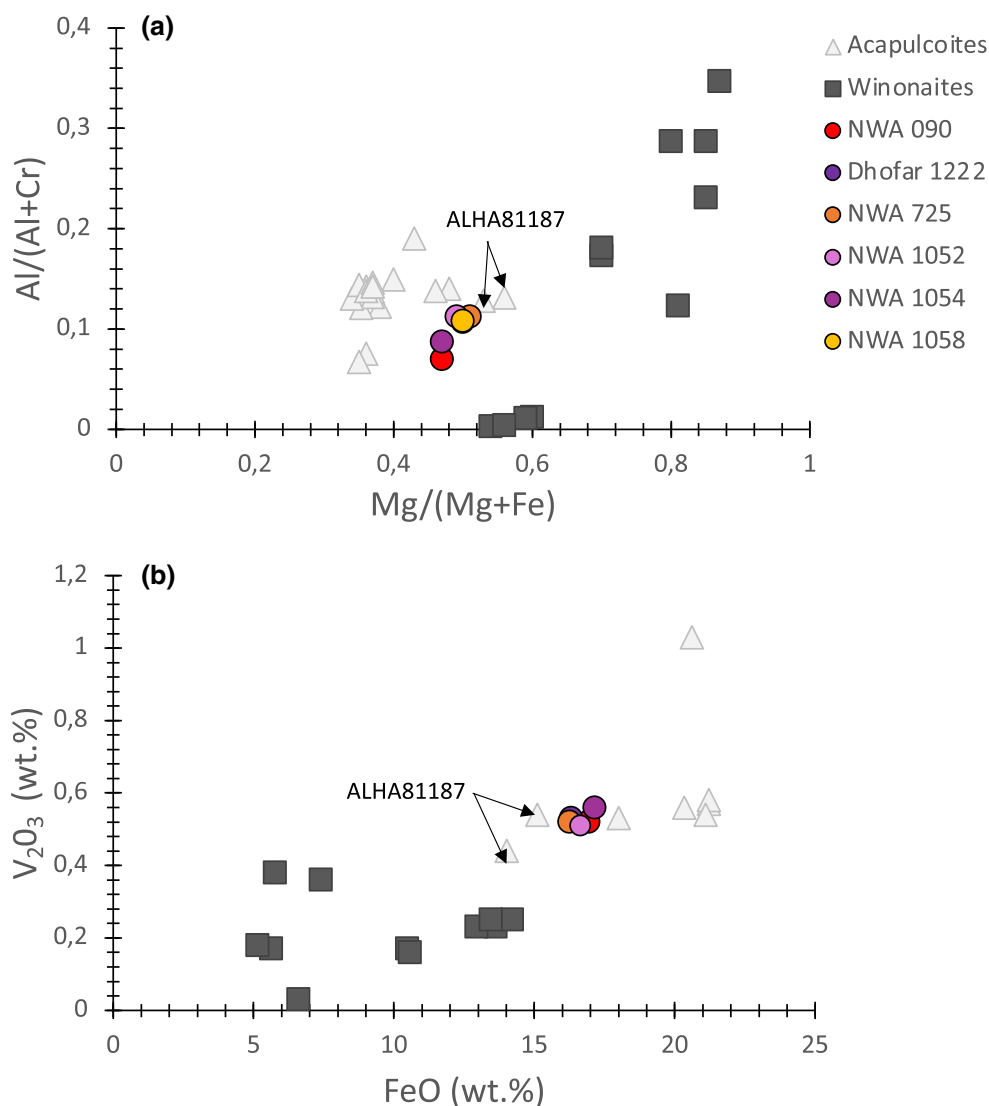


Fig. 9. Compositions of chromite in NWA 090, other classified relict chondrule-bearing winonaite, typical winonaite, and acapulcoite. (a) Mg/(Mg+Fe) versus Al/(Al+Cr) and (b) iron versus vanadium content of chromite. Data for acapulcoites are from Keil and McCoy (2018) and references therein. Data for winonaite are from Kimura et al. (1992) and Benedix et al. (2005). References and chromite compositions for Dhofar 1222, NWA 725, and NWA 1958 are listed in Table 4, along with NWA 090 opaque phases.

et al. (2019) and Farley et al. (2015) proposed that NWA 725 and NWA 8614, respectively, had sampled the chondritic protolith of the winonaite parent body, remained unaltered in the parent body's regolith. As such, they span the transition between winonaite and acapulcoites, as well as between primitive achondrites and highly metamorphosed chondrites.

Nonetheless, from a petrological point of view, that is, protogranular texture and abundant relict chondrules, and a mineralogic point of view, that is, olivine, low-Ca pyroxene, high-Ca pyroxene, and chromite composition, NWA 090, Dhofar 1222, NWA 725, NWA 1052 and its pairs NWA 1054, NWA 1058, NWA 1463, and NWA 8614

do not match the composition of typical winonaite and are rather close to acapulcoite characteristics. Oxygen isotopes have been referred as the only tool able to clearly distinguish between winonaite and acapulcoites (Benedix et al., 1998; Greenwood et al., 2012; Li et al., 2011). While NWA 090 entails an oxygen isotope signature that would attribute this primitive achondrite to the winonaite group rather than the acapulcoite–lodranite clan (Fig. 10), one should note that all the relict chondrule-bearing winonaite have  $\delta^{17}\text{O}$  and  $\delta^{18}\text{O}$  values lower than typical winonaite. This has already been highlighted by Greenwood et al. (2012). Indeed, the oxygen isotopic compositions of winonaite, treated by EATG for removing any terrestrial

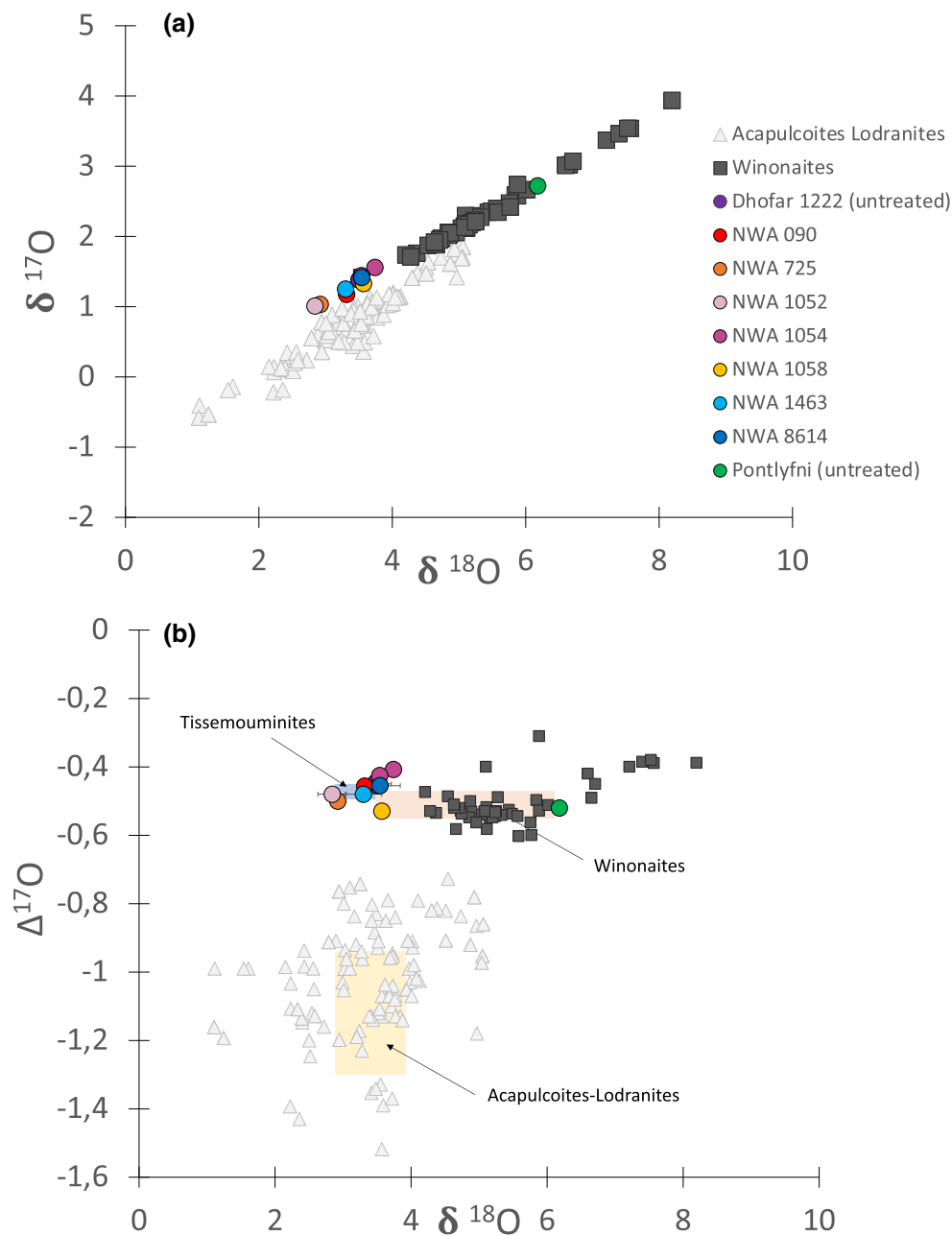


Fig. 10. Oxygen isotopes of primitive achondrites (a)  $\delta^{18}\text{O}$  versus  $\delta^{17}\text{O}$  in acapulcoites-lodranites, winonaites, and the classified chondritic winonaites. b) Oxygen variations ( $\delta^{18}\text{O}$  versus  $\Delta^{17}\text{O}$ ) in winonaites, acapulcoites-lodranites, and tissemmouminites. All the analyses plotted are for EATG-leached residues except for Dhofar 1222 and Pontlyfni which are untreated, and NWA 1054, NWA 1058 for which it is not specified. Colored boxes are average (1SD) of EATG residues for acapulcoites, winonaites, and five of the chondritic primitive achondrites (NWA 725, NWA 1052, NWA 1463, NWA 8614, and NWA 090) (NWA 090 are from this study; NWA 1058 are from Russell et al., 2003; NWA 1054 are from Irving Rumble, 2006; NWA 8614 from Farley et al., 2015; all other data are from Greenwood et al., 2012).

alteration, which is known to shift the isotopes, are  $\delta^{17}\text{O}$  of  $2.01 \pm 0.68\text{‰}$  (1SD),  $\delta^{18}\text{O}$  of  $4.81 \pm 1.29\text{‰}$  (1SD), and  $\Delta^{17}\text{O}$  of  $-0.51 \pm 0.04$  (1SD) (Greenwood et al., 2012). Considering the average of only EATG-treated samples, that is, NWA 725, NWA 1052, NWA 1463, NWA 8614, and NWA 090 (Table 6 and references therein), the oxygen

isotopic signatures for this group of primitive achondrites are narrowed to  $\delta^{17}\text{O}$  of  $1.18 \pm 0.17\text{‰}$ ,  $\delta^{18}\text{O}$  of  $3.18 \pm 0.30\text{‰}$ , and  $\Delta^{17}\text{O}$  of  $-0.47 \pm 0.02$ . This subgroup of primitive achondrites is resolvable in terms of their  $\delta^{18}\text{O}$  values from the typical winonaite oxygen isotopic compositions (Fig. 10), although plotting on the same



Table 6. Oxygen isotope signatures of primitive achondrites.

Meteorite	Weathering treatment	$\delta^{17}\text{O}_{\text{‰}}$	1 $\sigma$	$\delta^{18}\text{O}_{\text{‰}}$	1 $\sigma$	$\Delta^{17}\text{O}$	1 $\sigma$	References
NWA 725	EATG residue	1.03	0.05	2.92	0.11	-0.5	0.01	Greenwood et al. (2012)
NWA 1058	Not specified	1.33		3.57		-0.53		Russell et al. (2003)
NWA 1052	EATG residue	1.01	0.09	2.84	0.21	-0.48	0.01	Greenwood et al. (2012)
Dhofar 1222	Untreated	1.38	0.12	3.50	0.21	-0.45	0.01	Greenwood et al. (2012)
NWA 1054	Not specified	1.44		3.54		-0.43		Irving and Rumble (2006)
NWA 090	EATG residue	1.12		3.32		-0.46		This study
NWA 8614	EATG residue	1.42	0.17	3.54	0.30	-0.46	0.05	Farley et al. (2015)/MB
NWA 1463	EATG residue	1.25	0.15	3.3	0.27	-0.48	0	Greenwood et al. (2012)
Average ( $n = 8$ )		1.25		3.32		-0.47		
1 $\sigma$		0.17		0.29		0.03		
Average treated samples ( $n = 5$ )		1.18		3.18		-0.47		
1 $\sigma$		0.17		0.30		0.02		

oxygen isotopic fractionation line. The oxygen isotopic compositional similarities between different meteorite groups are not an unequivocal proxy for a common parent body origin, as best illustrated by the similarity of oxygen isotopes between the Earth, the Moon, aubrites, and enstatite chondrites (Dauphas et al., 2014) but rather suggest a common nebula reservoir of their parent bodies. Interestingly, the molybdenum (Mo) isotopic signature of NWA 725 is significantly different from winonaites (Worsham et al., 2017). Based on this discrepancy, Worsham et al. (2017) suggested NWA 725 and the rest of the winonaites to have sampled distinct parent bodies. This result, combined with oxygen isotopic data and petrographic, mineralogic, and geochemical information, suggests that NWA 090, Dhofar 1222, NWA 725, NWA 1052, NWA 1054, NWA 1058, NWA 1463, and NWA 8614 define a new group of primitive achondrites, transitional between winonaites and acapulcoites. We propose to name them tisseumouninites, in reference to the location village of Tisseumoumine, Morocco, where NWA 725 was found, NWA 725 being the first officially classified meteorite in *The Meteoritical Bulletin* (Grossman & Zipfel, 2001) with respect to the other members of this group.

### Classification Scheme of Primitive Achondrites

Since these classified chondritic primitive achondrites, aka tisseumouninites, conflict with the traditional dichotomy between acapulcoites and winonaites, we propose a revised criteria traditionally used for primitive achondrite classification (Benedix et al., 1998; Kimura et al., 1992; Li et al., 2011; Yugami et al., 1998). This will allow us to ascertain if, as proposed previously (Li et al., 2011), solely using the silicate mineralogy as a distinguishing criterion between primitive achondrites is risky, requiring the bulk oxygen isotopic composition as the only unambiguous way of

distinguishing primitive achondrites. One of the first criteria used is the Fa and Fs content of olivine and low-Ca pyroxene, respectively (Fig. 4). Kimura et al. (1992) defined winonaites with an  $\text{Fa} < \text{Fa}_6$ . As of now, acapulcoites and winonaites overlap in the  $\text{Fa}_{4-7}$  zone (Fig. 4), making this criterion probably the most confusing one for primitive achondrite classification. In fact, this criterion has led most of tisseumouninites to be classified as acapulcoites, then reclassified as winonaites while being in fact affiliated to a distinct primitive achondrite group (The *Meteoritical Bulletin* database). All winonaites have a  $\text{Fa} < \text{Fa}_7$  (Fig. 4). So far, tisseumouninites have an Fa content between  $\text{Fa}_{3,2}$  and  $\text{Fa}_{6,6}$  (Table 2 and references therein), that is, also less than  $\text{Fa}_7$ . This translates as a primitive achondrite; having an  $\text{Fa} > \text{Fa}_7$  is undeniably an acapulcoite. In fact, only seven classified acapulcoites yield Fa content lower than  $\text{Fa}_7$ , meaning they could be potential winonaite or tisseumouninite candidates: Yamato (Y) 983,237 ( $\text{Fa}_{6,7}$ ), NWA 4618 ( $\text{Fa}_{5,6}$ ), SuV 014 ( $\text{Fa}_{4,6}$ ), ALHA 81187 ( $\text{Fa}_{4,2}$ ) and its pairs ALH 84190 ( $\text{Fa}_{4,0}$ ), NWA 13041 ( $\text{Fa}_{4,1}$ ), and NWA 13839 ( $\text{Fa}_{3,8}$ ) (Keil & McCoy, 2018). The bulk oxygen isotopes of ALHA 81187 and ALH 84190 have identified them as acapulcoites while this information is lacking for the other samples. These seven acapulcoites will be discussed below through the criteria. Conversely, an  $\text{Fa} < \text{Fa}_{3,2}$  would be consistent with a winonaite affiliation. Between  $\text{Fa}_{3,2}$  and  $\text{Fa}_7$ , this criterion is not conclusive and should be used with caution.

Modal abundances of silicate minerals as well as phosphates and opaques are generally similar between lodranites, acapulcoites, and winonaites (Fig. 2). In fact, modal abundances of olivine, low-Ca pyroxene, and opaque minerals vary drastically within each of these three groups of primitive achondrites (cf. Zeng et al. [2019] and references therein). Kimura et al. (1992) have noted that the abundance ratios of olivine to orthopyroxene in

winonaites are generally lower than those of acapulcoites, but since then, discoveries of new winonaites have made this criterion nonconclusive. However, abundance ratios of olivine to opaque phases (i.e.,  $<0.8$ ) can be used to distinguish winonaites and tisseminites from the acapulcoite–lodranite clan, that is, a low abundance of olivine ( $<15$  wt%; acapulcoites ranging from 15 to 41 wt %; Keil & McCoy, 2018) together with a high opaque content ( $>30$  wt%; acapulcoites ranging from 1 to 27 wt%; Keil & McCoy, 2018) (Fig. 2a). That is, an olivine to opaque ratio lower than 0.8 will exclude an acapulcoite affiliation (Fig. 2b). It also follows that winonaites and tisseminites cannot be distinguished based on modal abundances alone, their modal abundances being extremely similar for all phases.

Kimura et al. (1992) have noted chemical composition differences between low-Ca pyroxenes, as well as high-Ca pyroxenes, in acapulcoites and winonaites. Low-Ca pyroxenes in winonaite tend to be FeO and MnO poorer than acapulcoites ones, while high-Ca pyroxenes are Na<sub>2</sub>O and Cr<sub>2</sub>O<sub>3</sub> poorer in winonaites compared to acapulcoites. As for modal abundances and Fa-Fs contents, the gap initially present between these two primitive meteorite clans has been filled, with more winonaites and acapulcoites analyzed (Fig. 6). As such, while the assertions made by Kimura et al. (1992) are in average still correct, some overlap occurred between low-Ca and high-Ca pyroxene chemical composition of acapulcoites and winonaites. Interestingly, the eight samples of interest, aka tisseminites, are intermediate in composition between acapulcoites and winonaites. As such, these minerals are not decisive proxies to distinguish between the three groups of primitive achondrites, except for extremely poor or low content of MnO and FeO content of low-Ca pyroxene, or extremely poor or rich content of Na<sub>2</sub>O, Cr<sub>2</sub>O<sub>3</sub>, Al<sub>2</sub>O<sub>3</sub>, and Mg# of high-Ca pyroxene (cf. Fig. 6). However, while plagioclase composition of acapulcoites and winonaites is indistinguishable, with composition of An<sub>2-31</sub>Ab<sub>67-88</sub>Or<sub>1.4-5.6</sub> and An<sub>5-52</sub>Ab<sub>48-91</sub>Or<sub>0.2-6.7</sub> for acapulcoites and winonaites, respectively (Keil & McCoy, 2018), tisseminites are typically enriched in K<sub>2</sub>O content (0.87–1.06 wt%; Fig. 6e) (Néri, 2019; Patzer et al., 2004; Zeng et al., 2019), yielding a range of composition of An<sub>12-14</sub>Ab<sub>80-83</sub>Or<sub>4.6-6.4</sub> (Table 3 and references therein). Similarly, vanadium composition of chromite can distinguish between winonaite and acapulcoite (Fig. 8) but will not discriminate the new group of primitive achondrites. One should note here that the number of primitive achondrite chromite composition in the literature is limited.

Olivine might be the most useful mineral to classify primitive achondrites. Indeed, FeO/MnO versus Fa content of olivine in acapulcoites and winonaites defines, remarkably, two trends (Fig. 5). As a matter of fact, the classified acapulcoites NWA 13041 and NWA 13839 plot

on the winonaite trend, concordant with their relatively low Fa-Fs contents (Fs<sub>4.6</sub> Fa<sub>3.8</sub>; Fs<sub>4.7</sub> Fa<sub>4.1</sub>, respectively). The acapulcoite ALHA 81187, while also being more reduced than typical acapulcoites, plots at the origin of the acapulcoite trend, also coherent with its acapulcoite oxygen isotopic signature. Surprisingly, winonaite NWA 4937 plots with the tisseminites along the acapulcoite trend, which does not match its oxygen isotopic composition (Weisberg et al., 2008). This FeO/MnO versus Fa content allows us to discriminate winonaite from the other two groups of primitive achondrites, apart from a few cases, but not tisseminites from acapulcoites. As such, we decided to combine olivine composition, that is, FeO/MnO ratio and Fa content, with plagioclase composition (Or content) in a ternary diagram to enable the classification of primitive achondrites (Fig. 11). Remarkably, the three groups of primitive achondrites can be clearly separated from one another. Classified acapulcoites NWA 13839 and NWA 13041 fit within winonaites. As such, we suggest a reclassification of NWA 13839 and NWA 13041 as winonaites. In fact, low-Ca pyroxene (Fs<sub>4.6</sub>; Fs<sub>4.7</sub>, respectively), olivine (Fa<sub>3.8</sub>, FeOMnO = 22.8; Fa<sub>4.1</sub>, FeOMnO = 18, respectively), and plagioclase compositions (An<sub>21.1</sub>Ab<sub>75.7</sub>Or<sub>3.2</sub>, An<sub>21</sub>Ab<sub>76</sub>Or<sub>3</sub>, respectively) (data from *The Meteoritical Bulletin*; Figs. 4–6 and 10) are evocative of winonaite affiliation rather than acapulcoite. Acapulcoite ALHA 81187, while being a highly reduced sample, lies consistently within the acapulcoite field. On the contrary, the classified winonaite NWA 4937 has oxygen isotopes in the range of winonaite but plots within the acapulcoite area (Fa<sub>7</sub>, FeO/MnO = 12.8, Or<sub>2.3</sub>) (Weisberg et al., 2008) (Figs. 4–6 and 10). As such, a thorough examination of this sample might be necessary since oxygen isotopic signature and chemistry are contradictory on its group affiliation. Few data are available for SuV 014 and NWA 4816, but investigation should be conducted to determine if they are indeed acapulcoites, winonaites, or tisseminites. The presence of relict chondrules in NWA 4816 might suggest a link to the tisseminite group, as well its FeO/MnO (12) and fayalite content (Fa<sub>5.6</sub>) of olivine (Weisberg et al., 2008) (Fig. 5). However, no data on plagioclase exists, which would enable the possibility to test its position in our classification scheme. Finally, winonaite NWA 6448 plots along the tisseminite newly defined group and examination should also be conducted to ascertain its correct classification. As such, we suggest detailed chemical analysis of primitive achondrite silicates for classification. This diagram demonstrates that systematic chemical composition of primitive achondrites permits a classification within winonaite, acapulcoite–lodranite, or tisseminite group, without the absolute need of oxygen isotopes.

Another criterion that could be used is the CRE age. As established by Eugster and Lorenzetti (2005), all measured acapulcoites and lodranites have CRE ages

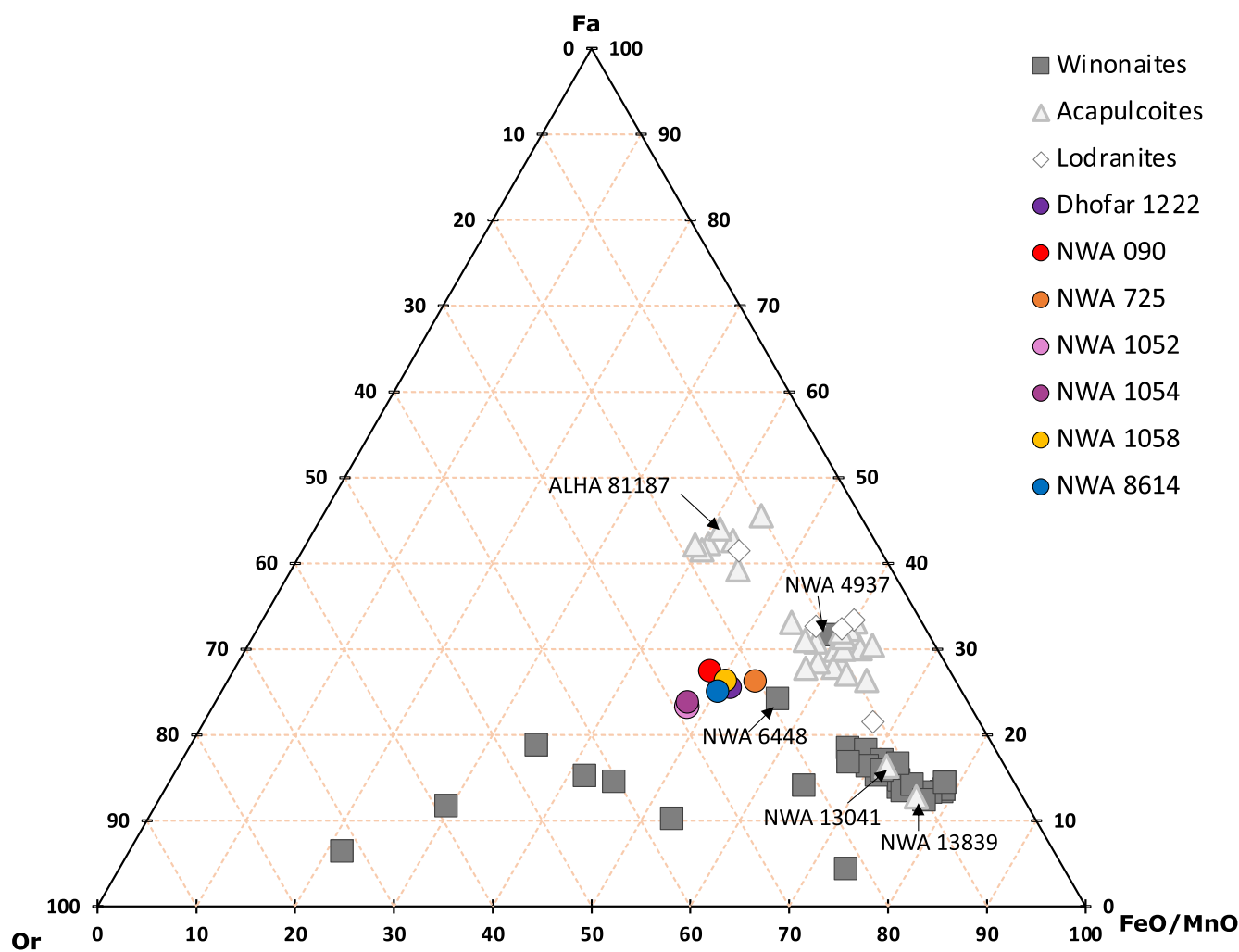


Fig. 11. Ternary diagram of mineral compositions in NWA 090, acapulcoites, and winonaites. The three endmembers represent Or content of plagioclase, Fa content of olivine, and FeO/MnO of olivine. Each value has been normalized to 100: for example, for the fayalite endmember, the equation is  $Fa/(Fa + Or + FeO/MnO) \times 100$ . As such, correlation observed in previous plots is artificially enhanced to observe the diverse groups of primitive achondrite compositions. NWA 090 and the other relict chondrule-bearing winonaites do indeed plot apart from both acapulcoites and winonaites. Data are from references in Figs. 4–6.

ranging between 4 and 7 Ma. NWA 1058 yields a CRE age of 38 Ma, which has led these authors to suggest a reclassification of this meteorite from acapulcoite to winonaite, since CRE ages of Winona, Pontlyfni, and Mount Morris range from 20 to 90 Ma (Benedix et al., 1998). However, few literature data are available, and this criterion cannot be used to distinguish tisseminites from winonaites.

Oxygen isotopes are often considered as the primary tool to distinguish between meteorite groups (Greenwood et al., 2012). Indeed, the three primitive achondrite groups, acapulcoite–lodranites, winonaites, and tisseminites, are resolvable from one another on a three-oxygen isotope plot (Fig. 10). This criterion has been argued to be the sole criterion that can accurately discriminate winonaites and

acapulcoites (Li et al., 2011). As highlighted by Greenwood et al. (2012, 2017), samples need to be pretreated for the removal of terrestrial weathering products. The absence of EATG treatment produces consequent shift in oxygen isotopes. In fact, when considering untreated samples, it is not possible to resolve tisseminites from winonaites. Moreover, they are on the same fractionation line. In any case, oxygen isotopes are not always measured to classify a meteorite. Here, we have demonstrated that a combination of olivine compositions, that is, FeO/MnO ratio and Fa content, with plagioclase compositions (Or content) enables the classification of meteorites within the three groups of primitive achondrites, and silicate elemental composition might be sufficient to accurately classify them.

### Petrogenesis of the Tissemouminite Parent Body

Based on the petrology, mineralogy, and chemistry of the eight hereby classified tisseminites, they most probably sampled regolith of a primitive achondrite parent body, being related to type 5/6 chondrites (Benedix et al., 2003; Floss et al., 2008; Zeng et al., 2019). Farley et al. (2015) have already proposed that various winonaite protoliths might have existed, due to the lack of Fe-Mg equilibrium between olivine and pyroxene in NWA 8614 (Fig. 4), arguing against a single metamorphic FeO reduction trend. This assertion is consistent with NWA 8614 being part of a newly defined primitive achondrite group. The lack of equilibrium between olivine and pyroxene Fe-Mg is in fact true for all the eight tisseminites (Fig. 4). More importantly, a recent study of Mo isotopes of IAB iron-complex meteorites and primitive achondrites has also suggested a minimum of three separate parent bodies (Worsham et al., 2017). The IAB iron-meteorite complex is characterized by the common presence of silicate inclusions and is classified in various groups (Wasson & Kallemeyn, 2002): the main group (MG) and five chemical subgroups (sLL, sLM, sLH, sHL, and sHH), defined by abundances of Au and Ni. The IAB-MG has been linked to the winonaite parent body, as a result of their similar petrography and common oxygen isotopic signature (Benedix et al., 2000; Clayton & Mayeda, 1996; Greenwood et al., 2012). Interestingly, while IAB MG iron meteorites and winonaites share a common Mo isotopic signature, supporting the proposed genetic link, the IAB sHH and IAB sHL have a distinct Mo isotopic composition. As such, they suggested that IAB MG and IAB sHH/sHL should have been derived from distinct parent bodies. Interestingly, NWA 725, now part of the tisseminite group, has a similar Mo isotopic composition to the IAB sHH/sHL, which could be seen as evidence for a common origin, although scarcity of information calls for caution in evaluating this potential genetic link (Worsham et al., 2017).

Nonetheless, metal-silicate Hf-W segregation model age estimated by Worsham et al. (2017) is  $3.4 \pm 0.7$  Ma after CAIs for IAB MG while ranging from 0.3 to 1.6 Ma CAIs for IAB sHH and IAB sHL. As such, IAB sHH and IAB sHL protoliths were formed during  $^{26}\text{Al}$  lifetime, when protoliths were melted to form metallic cores and silicate mantles (Bizzarro et al., 2005; Kleine et al., 2009). If a genetic link between IAB-sHH or IAB-sHL and tisseminites were to be demonstrated, these primitive achondrites would have formed before winonaites. The metallographic cooling rate of

$100 \text{ }^\circ\text{C Ma}^{-1}$  estimated for NWA 090 and NWA 1463 (Scott et al., 2014a) is in the range of winonaite cooling rates, that is,  $30\text{--}10^{3\text{--}4} \text{ }^\circ\text{C Ma}^{-1}$  (Goldstein et al., 2022; Scott et al., 2014a). In order to achieve these cooling rates before 2 Ma after CAI formation, these samples should have experienced extensive partial melting (Scott et al., 2014a; Worsham et al., 2017), which conflicts with the presence of relict chondrules. As such, either the tisseminite parent body formed later or it may have suffered subsequent disruption. For instance, it has been predicted that high velocity impacts of a 25-km radius projectile into very porous asteroids could cause heating to type 6 levels and cooling at rates of  $1\text{--}100 \text{ }^\circ\text{C Ma}^{-1}$  (Davison et al., 2012). As such, investigation of the potential genetic link between IAB sHH and/or IAB sHL with this new group of primitive achondrite would give hints into the petrogenesis of its parent body.

The protolith of tisseminite parent body was chondritic in nature, as evidence by the mineralogy and bulk composition that are intermediate between H and E chondrites, as for all primitive achondrites, and the presence of relict chondrules. While comparable to acapulcoites and winonaites, the chondritic precursor of tisseminites is not like any known chondritic group. However, its oxidation state and chemical composition put it closer to acapulcoites, while its oxygen isotopic composition relates it to the winonaite parent body. The variations in the temperatures of each of these meteorites are extremely similar, with a difference of temperature between olivine-chromite and 2-pyroxene thermometers of  $170 \pm 18 \text{ }^\circ\text{C}$ , and a narrow range of temperature estimated, that is  $\pm 20 \text{ }^\circ\text{C}$  of variation among samples. This indicates that these primitive achondrites have undergone a similar thermal history, which differs from the heterogeneous thermal history of winonaites (Benedix et al., 2005). As such, it means that either the thermal history of the tisseminite parent body was homogenous throughout or that these meteorites sampled a very narrow region of this parent body, as also suggested by their extremely similar compositions. However, while it has been argued that they could be paired (Irving & Rumble, 2006), their modal abundance variation prevents a pairing. As discussed previously, the oxygen fugacity of tisseminites is higher than the range observed in winonaites, although the number of data points is very limited (Benedix et al., 2005). They fit in the range calculated for acapulcoites, meaning that the oxidation state of their parent body is similar to that of the acapulcoite-lodranite parent body. It also means, as suggested previously by Righter and Drake (1996), that all primitive achondrites as well as HED and IAB irons have an  $f\text{O}_2$  approximately of 2 log units below the IW buffer and that the reservoir from which they formed

should have been homogenous. That corroborates the similarity of silicate and opaque phase compositions between the primitive achondrite groups and the difficulty of distinguishing and classifying them.

## CONCLUSION

NWA 090 and other relict chondrule-bearing winonaites, or chondritic winonaites (Dhofar 1222, NWA 725, NWA 1052, NWA 1054, NWA 1058, NWA 1463, NWA 8614), define a distinct group of primitive achondrites, the tisseouminites that most likely came from a distinct parent body compared to those of winonaites and acapulcoites, although sampling similar nebular material as winonaites in terms of oxygen isotopic composition. Their modal abundances and chemical compositions lie between acapulcoites and winonaites, conflicting with their traditional dichotomy. Nonetheless, by combining several chemical criteria, that is, fayalite content and FeO/MnO in olivines, as well as potassium content of plagioclases, these three groups of primitive achondrites can be clearly separated, highlighting the usefulness of mineral chemistry in primitive achondrite classification. In addition, oxygen isotopes, often cited as the only trustworthy criterion, confirm these eight samples to come from a distinct parent body than both winonaites and acapulcoites, hence also confirming the existence of this new tisseouminite group. Tisseouminites are pristine primitive achondrites, close to a petrographic type 5/6, as shown by the presence of relatively abundant relict chondrules and a closure temperature of metamorphism estimated at 820 °C. They probably sampled their parent body's regolith. Other samples, like NWA 4972, SuV 014, NWA 4816, and Y 983237, might be related to this group, and more information is needed to classify them with certainty. It is important to note that not all chemical information is available for all the samples, which sets some limit to this classification scheme. Classification of primitive achondrites, and in general achondrites, needs to provide detailed mineral chemistry of samples that permit an appropriate association to known or new meteorite groups.

*Acknowledgments*—We thank Arizona State University's Buseck Center for Meteorite Studies (BCMS) for the loan of the meteorite sample NWA 090. We are grateful to Laura Chiarantini and Tiziano Catelani for SEM work in the University of Florence and Ken Dominik for EMPA assistance at the University of Arizona. A.S. thanks Enrico Bruschini. The reviewer is thanked for his insightful feedback and suggestions, and we thank Timothy A.J. Jull for editorial handling. This work is supported by the EU's Horizon 2020 research and

innovation program under the Marie Skłodowska-Curie grant agreement n°884029 to A.S. J.D. was supported by BCMS. C.C., E.B., G.P., and T.C. were partially supported by ASI INAF agreement n.2018-16-HH.0, OLBODIES project. MA, RCG, and IAF also acknowledge support from a UK Science and Technology Facilities Council Grant (grant #ST/P000657/1).

*Data Availability Statement*—The data that support the findings of this study are available in the tables of this article.

*Editorial Handling*—Dr. A. J. Timothy Jull

## REFERENCES

- Benedix, G. K., and Lauretta, D. S. 2006. Thermodynamic Constraints on the Formation History of Acapulcoites (Abstract #2129). 37th Lunar and Planetary Science Conference. CD-ROM.
- Benedix, G. K., Lauretta, D. S., and McCoy, T. J. 2005. Thermodynamic Constraints on the Formation Conditions of Winonaites and Silicate-Bearing IAB Irons. *Geochimica et Cosmochimica Acta* 69: 5123–31. <https://doi.org/10.1016/j.gca.2005.03.048>.
- Benedix, G. K., McCoy, T. J., Keil, K., Bogard, D. D., and Garrison, D. H. 1998. A Petrologic and Isotopic Study of Winonaites: Evidence for Early Partial Melting, Brecciation, and Metamorphism. *Geochimica et Cosmochimica Acta* 62: 2535–53. [https://doi.org/10.1016/S0016-7037\(98\)00166-5](https://doi.org/10.1016/S0016-7037(98)00166-5).
- Benedix, G. K., McCoy, T. J., Keil, K., and Love, S. G. 2000. A Petrologic Study of the IAB Iron Meteorites: Constraints on the Formation of the IAB-Winonaite Parent Body. *Meteoritics & Planetary Science* 35: 1127–41.
- Benedix, G. K., McCoy, T. J., and Lauretta, D. S. 2003. Is NWA 1463 the Most Primitive Winonaite? 66th Annual Meteoritical Society Meeting, abstract 5125.
- Bevan, A. W. R., and Grady, M. M. 1988. Mount Morris (Wisconsin): A Fragment of the IAB Iron Pine River? *Meteoritics* 23: 349–52.
- Bizzarro, M., Baker, J. A., Haack, H., and Lundgaard, K. L. 2005. Rapid Timescales for Accretion and Melting of Differentiated Planetesimals Inferred from  $^{26}\text{Al}$ - $^{26}\text{Mg}$  Chronometry. *The Astrophysical Journal* 632: L41–4.
- Bouvier, A., Gattacceca, J., Grossman, J., and Metzler, K. 2017. The Meteoritical Bulletin, No. 105. *Meteoritics & Planetary Science* 52: 2411. <https://doi.org/10.1111/maps.12944>.
- Cecchi, V., and Caporali, S. 2015. Petrologic and Minerochemical Trends of Acapulcoites, Winonaites and Lodranites: New Evidence from Image Analysis and EMPA Investigations. *Geosciences* 5: 222–42. <https://doi.org/10.3390/geosciences5030222>.
- Clayton, R. N., and Mayeda, T. K. 1996. Oxygen Isotope Studies of Achondrites. *Geochimica et Cosmochimica Acta* 60: 1999–2017. [https://doi.org/10.1016/0016-7037\(96\)00074-9](https://doi.org/10.1016/0016-7037(96)00074-9).
- Dauphas, N., Burkhardt, C., Warren, P. H., and Teng, F.-Z. 2014. Geochemical Arguments for Earth-Like Moonforming Impactor. *Philosophical Transactions of the Royal Society A* 372: 20130244.

- Davis, A., Ganapathy, R., and Grossman, L. 1977. Pontlyfni: A Differentiated Meteorite Related to the Group IAB Irons. *Earth and Planetary Science Letters* 35: 19–24. [https://doi.org/10.1016/0012-821X\(77\)90023-1](https://doi.org/10.1016/0012-821X(77)90023-1).
- Davison, T. M., Ciesla, F. J., and Collins, G. S. 2012. Post-Impact Thermal Evolution of Porous Planetesimals. *Geochimica et Cosmochimica Acta* 95: 252–69. <https://doi.org/10.1016/j.gca.2012.08.001>.
- Eugster, O., and Lorenzetti, S. 2005. Cosmic-Ray Exposure Ages of Four Acapulcoites and Two Differentiated Achondrites and Evidence for a Two-Layer Structure of the Acapulcoite/Lodranite Parent Asteroid. *Geochimica et Cosmochimica Acta* 69: 2675–85. <https://doi.org/10.1016/j.gca.2004.12.006>.
- Farley, K., Ruzicka, A. M., and Armstrong, K. 2015. NWA 8614: The Least Heated Winonaite, 46th Lunar and Planetary Science Conference, Houston, TX, abstract 1821.
- Floss, C. 2000. Complexities on the Acapulcoite-Lodranite Parent Body: Evidence from Trace Element Distributions in Silicate Minerals. *Meteoritics & Planetary Science* 35: 1073–85. <https://doi.org/10.1111/j.1945-5100.2000.tb01494.x>.
- Floss, C., Crozaz, G., Jolliff, B., Benedix, G., and Colton, S. 2008. Evolution of the Winonaite Parent Body: Clues from Silicate Mineral Trace Element Distributions. *Meteoritics & Planetary Science* 43: 657–74. <https://doi.org/10.1111/j.1945-5100.2008.tb00676.x>.
- Friedrich, J. M., Weisberg, M. K., Ebel, D. S., Biltz, A. E., Corbett, B. M., Iotzov, I. V., Khan, W. S., and Wolman, M. D. 2015. Chondrule Size and Related Physical Properties: A Compilation and Evaluation of Current Data Across all Meteorite Groups. *Geochemistry* 75: 419–43. <https://doi.org/10.1016/j.chemer.2014.08.003>.
- Gardner-Vandy, K. G., Lauretta, D. S., Greenwood, R. C., McCoy, T. J., Killgore, M., and Franchi, I. A. 2012. The Tafassasset Primitive Achondrite: Insights into Initial Stages of Planetary Differentiation. *Geochimica et Cosmochimica Acta* 85: 142–59. <https://doi.org/10.1016/j.gca.2012.01.014>.
- Goldstein, J. I., Scott, E. R. D., Winfield, T. B., Yang, J., and Rubin, A. 2022. Cooling Rates and Impact Histories of Group IAB and Other IAB Complex Iron Meteorites Inferred from Zoned Taenite and the Cloudy Zone. *Meteoritics & Planetary Science* 57: 238–60. <https://doi.org/10.1111/maps.13745>.
- Gooding, J. L., and Keil, K. 1981. Relative Abundances of Chondrule Primary Textural Types in Ordinary Chondrites and their Bearing on Conditions of Chondrule Formation. *Meteoritics* 16: 17–43. <https://doi.org/10.1111/j.1945-5100.1981.tb00183.x>.
- Graham, A. L., Easton, A. J., and Hutchison, R. 1977. Forsterite Chondrites; the Meteorites Kakangari, Mount Morris (Wisconsin, Pontlyfni, and Winona). *Mineralogical Magazine* 41: 210.
- Greenwood, R. C., Burbine, T. H., Miller, M. F., and Franchi, I. A. 2017. Melting and Differentiation of Early-Formed Asteroids: The Perspective from High Precision Oxygen Isotope Studies. *Geochemistry* 77: 1–43. <https://doi.org/10.1016/j.chemer.2016.09.005>.
- Greenwood, R. C., Franchi, I. A., Gibson, J. M., and Benedix, G. K. 2012. Oxygen Isotope Variation in Primitive Achondrites: The Influence of Primordial, Asteroidal and Terrestrial Processes. *Geochimica et Cosmochimica Acta* 94: 146–63. <https://doi.org/10.1016/j.gca.2012.06.025>.
- Grossman, J. N., and Zipfel, J. 2001. The Meteoritical Bulletin. *Meteoritics & Planetary Science* 36: 1293–322.
- Huebner, J. S., and Nord, G. L. 1981. Assessment of Diffusion in Pyroxenes: What We Do and Do Not Know. *Lunar and Planetary Science Conference* 12: 479–81.
- Hunt, A. C., Benedix, G. K., Hammond, S. J., Bland, P. A., Rehkämper, M., Kreissig, K., and Strekopytov, S. 2017. A Geochemical Study of the Winonaite: Evidence for Limited Partial Melting and Constraints on the Precursor Composition. *Geochimica et Cosmochimica Acta* 199: 13–30. <https://doi.org/10.1016/j.gca.2016.10.043>.
- Huss, G. R., Rubin, A. E., and Grossman, J. N. 2006. Thermal Metamorphism in Chondrites. In *Meteorites and the Early Solar System II*, edited by Lauretta D. and McSween H. Y. Tucson: University of Arizona Press. pp. 567–86.
- Irving, A. J., and Rumble, D. 2006. Oxygen Isotopes in Brachina, SAH 99555 and Northwest Africa 1054. 69th Annual Meteoritical Society Meeting, 5288.
- Keil, K., and McCoy, T. J. 2018. Acapulcoite-Lodranite Meteorites: Ultramafic Asteroidal Partial Melt Residues. *Geochemistry* 78: 153–203. <https://doi.org/10.1016/j.chemer.2017.04.004>.
- Kimura, M., Tsuchiyama, A., Fukuora, T., and Iimura, Y. 1992. Antarctic Primitive Achondrites, Yamato-74025, -75300, and -75305: Their Mineralogy, Thermal History, and the Relevance to Winonaite. *Proceedings of the NIPR Symposium on Antarctic Meteorites* 5: 165–90.
- Kleine, T., Touboul, M., Bourdon, B., Nimmo, F., Mezger, K., Palme, H., Jacobsen, S. B., Yin, Q.-Z., and Halliday, A. N. 2009. Hf–W Chronology of the Accretion and Early Evolution of Asteroids and Terrestrial Planets. *Geochimica et Cosmochimica Acta* 73: 5150–88. <https://doi.org/10.1016/j.gca.2008.11.047>.
- Kovach, H. A., and Jones, R. H. 2010. Feldspar in Type 4–6 Ordinary Chondrites: Metamorphic Processing on the H and LL Chondrite Parent Bodies. *Meteoritics and Planetary Science* 45: 246–64.
- Krot, A. N., Keil, K., Scott, E. R. D., Goodrich, C. A., and Weisberg, M. K. 2014. Classification of Meteorites and Their Genetic Relationships. In *Treatise on Geochemistry*, edited by Holland H. D. and Turekain K. K. Amsterdam, Edinburgh, Alpha: Elsevier. pp. 1–63. <https://doi.org/10.1016/B978-0-08-095975-7.00102-9>.
- Kullerud, G. 1963. The Fe–Ni–S System. *Annual Report of the Geophysical Laboratory* 67: 4055–61.
- Lanari, P., Vidal, O., De Andrade, V., Dubacq, B., Lewin, E., Grosch, E. G., and Schwartz, S. 2014. XMapTools: A MATLAB®-Based Program for Electron Microprobe X-Ray Image Processing and Geothermobarometry. *Computers & Geosciences* 62: 227–40. <https://doi.org/10.1016/j.cageo.2013.08.010>.
- Li, S., Wang, S., Bao, H., Miao, B., Liu, S., Coulson, I. M., Li, X., and Li, Y. 2011. The Antarctic Achondrite, Grove Mountains 021663: An Olivine-Rich Winonaite. *Meteoritics & Planetary Science* 46: 1329–44. <https://doi.org/10.1111/j.1945-5100.2011.01232.x>.
- McCoy, T. J., Keil, K., Clayton, R. N., Mayeda, T. K., Bogard, D. D., Garrison, D. H., Huss, G. R., Hutcheon, I. D., and Wieler, R. 1996. A Petrologic, Chemical, and Isotopic Study of Monument Draw and Comparison with Other Acapulcoites: Evidence for Formation by Incipient Partial Melting. *Geochimica et Cosmochimica Acta* 60: 2681–708. [https://doi.org/10.1016/0016-7037\(96\)00109-3](https://doi.org/10.1016/0016-7037(96)00109-3).

- McCoy, T. J., Keil, K., Clayton, R. N., Mayeda, T. K., Bogard, D. D., Garrison, D. H., and Wieler, R. 1997. A Petrologic and Isotopic Study of Lodranites: Evidence for Early Formation as Partial Melt Residues from Heterogeneous Precursors. *Geochimica et Cosmochimica Acta* 61: 623–37. [https://doi.org/10.1016/S0016-7037\(96\)00359-6](https://doi.org/10.1016/S0016-7037(96)00359-6).
- McCoy, T. J., Keil, K., Muenow, D. W., and Wilson, L. 1997. Partial Melting and Melt Migration in the Acapulcoite-Lodranite Parent Body. *Geochimica et Cosmochimica Acta* 61: 639–50. [https://doi.org/10.1016/S0016-7037\(96\)00365-1](https://doi.org/10.1016/S0016-7037(96)00365-1).
- McSween, H. Y., Jr., Ghosh, A., Grimm, R. E., Wilson, L., and Young, E. D. 2002. Thermal Evolution Models of Asteroids. In *Asteroids III*, edited by Bottke Jr. W. F., Cellino A., Paolicchi P. and Binzel R. P. Tucson: University of Arizona Press. pp. 559–71.
- Mercier, J.-C., and Nicolas, A. 1975. Textures and Fabrics of Upper-Mantle Peridotites as Illustrated by Xenoliths from Basalts. *Journal of Petrology* 16: 454–87.
- Miller, M. F., Franchi, I. A., Thiemens, M. H., Jackson, T. L., Brack, A., Kurat, G., and Pillinger, C. T. 2002. Mass-Independent Fractionation of Oxygen Isotopes During Thermal Decomposition of Carbonates. *Proceedings of the National Academy of Sciences of the United States of America* 99: 10988–93. <https://doi.org/10.1073/pnas.172378499>.
- Mittlefehldt, D. W. 2014. Achondrites. In *Treatise on Geochemistry*, edited by Holland H. D. and Turekain K. K. Amsterdam, Edinburgh, Alpha: Elsevier. pp. 235–66. <https://doi.org/10.1016/B978-0-08-095975-7.00108-X>.
- Mittlefehldt, D. W., Lindstrom, M. M., Bogard, D. D., Garrison, D. H., and Field, S. W. 1996. Acapulco- and Lodran-Like Achondrites: Petrology, Geochemistry, Chronology, and Origin. *Geochimica et Cosmochimica Acta* 60: 867–82. [https://doi.org/10.1016/0016-7037\(95\)00423-8](https://doi.org/10.1016/0016-7037(95)00423-8).
- Morse, S. A. 1980. *Basalts and Phase Diagrams*. New York: Springer. <https://doi.org/10.1007/978-1-4612-6081-3>.
- Néri, A. 2019. *Metal-Silicate Differentiation in Early-Accreted Small Bodies of the Solar System: A Multidisciplinary Approach*. PhD thesis, Solar and Stellar Astrophysics [astro-ph.SR]. Université Paul Sabatier - Toulouse III. NNT: 2019TOU30184.
- Neumann, W., Henke, S., Breuer, D., Gail, H.-P., Schwarz, W. H., Tieloff, M., Hopp, J., and Spohn, T. 2018. Modeling the Evolution of the Parent Body of Acapulcoites and Lodranites: A Case Study for Partially Differentiated Asteroids. *Icarus* 311: 146–69. <https://doi.org/10.1016/j.icarus.2018.03.024>.
- Palme, H., Schultz, L., Spettel, B., Weber, H. W., Wänke, H., Michel-Levy, M. C., and Lorin, J. C. 1981. The Acapulco Meteorite: Chemistry, Mineralogy and Irradiation Effects. *Geochimica et Cosmochimica Acta* 45: 727–52. [https://doi.org/10.1016/0016-7037\(81\)90045-4](https://doi.org/10.1016/0016-7037(81)90045-4).
- Patzer, A., Hill, D. H., and Boynton, W. V. 2004. Evolution and Classification of Acapulcoites and Lodranites from a Chemical Point of View. *Meteoritics & Planetary Science* 39: 61–85. <https://doi.org/10.1111/j.1945-5100.2004.tb00050.x>.
- Prinz, M., Nehru, C. E., Delaney, J. S., and Weisberg, M. 1983. Silicates in IAB and IIICD Irons, Winonaites, Lodranites and Brachina: A Primitive and Modified-Primitive Group (Abstract). 14th Lunar and Planetary Science Conference. pp. 616–7.
- Righter, K., and Drake, M. J. 1996. Core Formation in Earth's Moon, Mars, and Vesta. *Icarus* 124: 513–29. <https://doi.org/10.1006/icar.1996.0227>.
- Righter, K., Sutton, S. R., Danielson, L., Pando, K., and Neville, M. 2016. Redox Variations in the Inner Solar System with New Constraints from Vanadium XANES in Spinels. *American Mineralogist* 101: 1928–42. <https://doi.org/10.2138/am-2016-5638>.
- Rubin, A. E. 2007. Petrogenesis of Acapulcoites and Lodranites: A Shock-Melting Model. *Geochimica et Cosmochimica Acta* 71: 2383–401. <https://doi.org/10.1016/j.gca.2007.02.010>.
- Russell, S. S., Zipfel, J., Folco, L., Jones, R., Grady, M. M., McCoy, T., and Grossman, J. N. 2003. Meteoritical Bulletin, No. 87. *Meteoritics & Planetary Science* 38: A189–248.
- Sack, R. O., and Ghiorso, M. S. 1991. Chromian Spinels as Petrogenetic Indicators: Thermodynamics and Petrological Applications. *American Mineralogist* 76: 827–47.
- Schrader, D. L., McCoy, T. J., and Gardner-Vandy, K. 2017. Relict Chondrules in Primitive Achondrites: Remnants from their Precursor Parent Bodies. *Geochimica et Cosmochimica Acta* 205: 295–312. <https://doi.org/10.1016/j.gca.2017.02.012>.
- Schulz, T., Münker, C., Mezger, K., and Palme, H. 2010. Hf–W Chronometry of Primitive Achondrites. *Geochimica et Cosmochimica Acta* 74: 1706–18. <https://doi.org/10.1016/j.gca.2009.12.016>.
- Scott, E. R. D., and Krot, A. N. 2014. Chondrites and Their Components. In *Treatise on Geochemistry*, edited by Holland H. D. and Turekain K. K. Amsterdam, Edinburgh, Alpha: Elsevier. pp. 65–137. <https://doi.org/10.1016/B978-0-08-095975-7.00104-2>.
- Scott, E. R. D., Krot, T. V., Goldstein, J. I., and Benedix, G. K. 2014a. Thermal and Impact Histories and Origin of Winonaites and IAB Iron Meteorites. 77th Annual Meteoritical Society Meeting. p. 5107.
- Scott, E. R. D., Krot, T. V., Goldstein, J. I., and Wakita, S. 2014b. Thermal and Impact History of the H Chondrite Parent Asteroid During Metamorphism: Constraints from Metallic Fe–Ni. *Geochimica et Cosmochimica Acta* 136: 13–37. <https://doi.org/10.1016/j.gca.2014.03.038>.
- Starkey, N. A., Jackson, C. R. M., Greenwood, R. C., Parman, S., Franchi, I. A., Jackson, M., Fitton, J. G., Stuart, F. M., Kurz, M., and Larsen, L. M. 2016. Triple Oxygen Isotopic Composition of the High-<sup>3</sup>He/<sup>4</sup>He Mantle. *Geochimica et Cosmochimica Acta* 176: 227–38. <https://doi.org/10.1016/j.gca.2015.12.027>.
- Taylor, G. J., Maggiore, P., Scott, E. R. D., Rubin, A. E., and Keil, K. 1987. Original Structures, and Fragmentation and Reassembly Histories of Asteroids: Evidence from Meteorites. *Icarus* 69: 1–13.
- Tomkins, A. G., Johnson, T. E., and Mitchell, J. T. 2020. A Review of the Chondrite–Achondrite Transition, and a Metamorphic Facies Series for Equilibrated Primitive Stony Meteorites. *Meteoritics & Planetary Science* 55: 857–85. <https://doi.org/10.1111/maps.13472>.
- Van Schmus, W. R., and Wood, J. A. 1967. A Chemical-Petrologic Classification for the Chondritic Meteorites. *Geochimica et Cosmochimica Acta* 31: 747–65. [https://doi.org/10.1016/S0016-7037\(67\)80030-9](https://doi.org/10.1016/S0016-7037(67)80030-9).
- Wadhwa, M. 2008. Redox Conditions on Small Bodies, the Moon and Mars. *Reviews in Mineralogy and Geochemistry* 68: 493–510. <https://doi.org/10.2138/rmg.2008.68.17>.
- Wasson, J. T., and Kallemeyn, G. W. 2002. The IAB Iron-Meteorite Complex: A Group, Five Subgroups, Numerous Grouplets, Closely Related, Mainly Formed by Crystal Segregation in Rapidly Cooling Melts. *Geochimica et*

- Cosmochimica Acta* 66: 2445–73. [https://doi.org/10.1016/S0016-7037\(02\)00848-7](https://doi.org/10.1016/S0016-7037(02)00848-7).
- Weisberg, M. K., McCoy, T. J., and Krot, A. N. 2006. Systematics and Evaluation of Meteorite Classification. In *Meteorites and the Early Solar System II*, edited by Lauretta D. S. and McSween H. Y. Tucson, Arizona: University of Arizona Press. pp. 19–52.
- Weisberg, M. K., Smith, C., Benedix, G. K., Folco, L., Righter, K., Zipfel, J., Yamaguchi, A., and Chennaoui Aoudjehane, H. 2008. The Meteoritical Bulletin. *Meteoritics & Planetary Science* 43: 1551–88.
- Willis, J., and Goldstein, J. I. 1981. A Revision of Metallographic Cooling Rate Curves for Chondrites (Abstract). 12th Lunar and Planetary Science Conference. pp. 1135–43.
- Wlotzka, F. 1993. A Weathering Scale for the Ordinary Chondrites. *Meteoritics* 28: 460.
- Wood, J. A. 1967. Chondrites: Their Metallic Minerals, Thermal Histories, and Parent Planets. *Icarus* 6: 1–49.
- Worsham, E. A., Bermingham, K. R., and Walker, R. J. 2017. Characterizing Cosmochemical Materials with Genetic Affinities to the Earth: Genetic and Chronological Diversity Within the IAB Iron Meteorite Complex. *Earth and Planetary Science Letters* 467: 157–66. <https://doi.org/10.1016/j.epsl.2017.02.044>.
- Yugami, K., Takeda, H., Kojima, H., and Miyamoto, M. 1998. Modal Mineral Abundances and the Differentiation Trends in Primitive Achondrites. *Antarctic Meteorite Research* 11: 49–70.
- Zeng, X., Shang, Y., Li, S., Li, X., Wang, S., and Li, Y. 2019. The Layered Structure Model for Winonaite Parent Asteroid Implicated by Textural and Mineralogical Diversity. *Earth Planets Space* 71: 38. <https://doi.org/10.1186/s40623-019-1015-9>.
-